

The transgenic expression of LARGE exacerbates the muscle phenotype of dystroglycanopathy mice.

Journal:	<i>Human Molecular Genetics</i>
Manuscript ID:	HMG-2013-D-01094.R1
Manuscript Type:	2 General Article - UK Office
Date Submitted by the Author:	08-Nov-2013
Complete List of Authors:	Whitmore, Charlotte; Royal Veterinary College, Comparative Biomedical Sciences Fernandez-Fuente, Marta; Royal Veterinary College, Comparative Biomedical Sciences Booler, Helen; Royal Veterinary College, Comparative Biomedical Sciences Parr, Callum; Royal Veterinary College, Comparative Biomedical Sciences Kavishwar, Manoli; Royal Veterinary College, Comparative Biomedical Sciences Ashraf, Attia; Royal Veterinary College, Comparative Biomedical Sciences Lacey, Erica; Royal Veterinary College, Comparative Biomedical Sciences Kim, Jihee; Royal Veterinary College, Comparative Biomedical Sciences Terry, Rebecca; Royal Veterinary College, Comparative Biomedical Sciences Wells, Kim; Royal Veterinary College, Comparative Biomedical Sciences Muntoni, Francesco; Institute of Child Health, UCL, Dubowitz Neuromuscular Unit Wells, Dominic; Royal Veterinary College, Comparative Biomedical Sciences Brown, Sue; Royal Veterinary College, Comparative Biomedical Sciences
Key Words:	dystroglycan, fukutin related protein, LARGE, muscular dystrophy

1
2
3 The transgenic expression of LARGE exacerbates the muscle phenotype of dystroglycanopathy
4
5
6 mice.
7
8
9

10
11 Charlotte Whitmore^{1,2*}, Marta Fernandez-Fuente^{1*}, Helen Booler¹, Callum Parr¹, Manoli
12 Kavishwar¹, Attia Ashraf³, Erica Lacey¹, Jihee Kim¹, Rebecca Terry¹, Mark. R. Ackroyd¹, Kim
13
14 E. Wells¹, Francesco.Muntoni³, Dominic J. Wells¹, Susan C. Brown*¹.
15
16
17

18
19
20 ¹ Comparative Biomedical Sciences, Royal Veterinary College, University of London, ²Division
21 of Brain Sciences, Department of Medicine, Imperial College London, ³ Dubowitz
22 Neuromuscular Unit, Institute of Child Health, UCL.
23
24
25
26
27
28
29
30

31 Address for correspondence: S.C.Brown (020 7468 1212, scbrown@rvc.ac.uk) - Comparative
32 Biomedical Sciences, Royal Veterinary College, London, United Kingdom NW1 0TU.
33
34
35
36
37
38
39
40
41
42
43
44
45
46
47
48
49
50
51
52

53 *The authors wish it to be known that, in their opinion, the first two authors should be regarded
54 as joint First Authors.
55
56
57
58
59
60

Abstract.

1
2
3
4
5
6
7
8
9
10
11
12
13
14
15
16
17
18
19
20
21
22
23
24
25
26
27
28
29
30
31
32
33
34
35
36
37
38
39
40
41
42
43
44
45
46
47
48
49
50
51
52
53
54
55
56
57
58
59
60

Mutations in fukutin related protein (FKRP) underlie a group of muscular dystrophies associated with the hypoglycosylation of α -dystroglycan (α -DG), a proportion of which show central nervous system involvement. Our original FKRP knock down mouse (FKRP^{KD}) replicated many of the characteristics seen in patients at the severe end of the dystroglycanopathy spectrum but died perinatally precluding its full phenotyping and use in testing potential therapies. We have now overcome this by crossing FKRP^{KD} mice with those expressing Cre recombinase under the Sox1 promoter. Due to our original targeting strategy this has resulted in the restoration of Fkrp levels in the central nervous system but not the muscle, thereby generating a new model (FKRP_{MD}) which develops a progressive muscular dystrophy resembling what is observed in limb girdle muscular dystrophy. Like-acetylglucosaminyltransferase (LARGE) is a bifunctional glycosyltransferase previously shown to hyperglycosylate α -dystroglycan. In order to investigate the therapeutic potential of LARGE up-regulation we have now crossed the FKRP_{MD} line with one overexpressing LARGE and show that, contrary to expectation, this results in a worsening of the muscle pathology implying that any future strategies based upon LARGE up-regulation require careful management.

Introduction.

Dystroglycan (DG) forms the central component of the dystrophin associated protein complex and has been attributed with a primary role in the deposition, organisation and turnover of basement membranes (1-7). It is composed of two subunits, both of which are encoded by the *DAG1* gene: β -DG, a transmembrane protein and α -DG, a highly glycosylated peripheral membrane protein (1). The primary sequence of α -DG predicts a molecular mass of 72kDa: however, due to extensive post-translational glycosylation the final molecular weight is around 156kDa in skeletal muscle (8). The O-linked glycan chains of the central mucin domain of α -DG mediate binding to basement membrane ligands including laminin (9), perlecan (10) agrin (11-13), neuexin in the brain (14), pikachurin in the eye (15) and Slit (16) by interaction with the laminin LG (laminin globular) domains (17,18) and their loss from the central mucin domain of α -DG is considered to be central to the pathogenesis of a subgroup of congenital muscular dystrophies (CMDs), the dystroglycanopathies (7,19-21).

To date at least 15 genes have been implicated in the glycosylation and/or processing of α DG, which now include *POMT1* (*PROTEIN O-MANNOSYL-TRANSFERASE 1*) (22), *POMT2* (*PROTEIN O-MANNOSYL-TRANSFERASE 2*) (23), *POMGNT1* (*PROTEIN O-MANNOSE BETA-1,2-N-ACETYLGLUCOSAMINYLTRANSFERASE*) (24), *LARGE* (25-27), *FKT* (*FUKUTIN*) (28), *FKRP* (29,30), *DPM2* (*DOLICHYL-PHOSPHATE MANNOSYLTRANSFERASE POLYPEPTIDE 2*), *DPM3* (*DOLICHYL-PHOSPHATE MANNOSYLTRANSFERASE POLYPEPTIDE 3*) (31), *ISPD* (*ISOPRENOID SYNTHASE DOMAIN CONTAINING*) (32,33), *GTDC2* (*GLYCOSYLTRANSFERASE-LIKE DOMAIN*

1
2
3 CONTAINING 2) (34), *TMEM5* (TRANSMEMBRANE PROTEIN 5) (35), *B3GNT1* (BETA-1,3-N-
4 ACETYLGLUCOSAMINYLTRANSFERASE 1) (36), *DOLK* (DOLICHOL KINASE) (37),
5
6
7
8 *SGK196* (SUGEN KINASE 196) (38) and *GMPPB* (GDP-MANNOSE PYROPHOSPHORYLASE
9
10 *B*) (39). Mutations in these genes are often associated with a wide clinical spectrum of
11
12 phenotypes, including severe CMD and structural brain defects as exemplified by Walker
13
14 Warburg syndrome (WWS) OMIM 236670, Muscle Eye Brain disease (MEB) OMIM 253280,
15
16 Fukuyama CMD (FCMD) OMIM 253800, and congenital muscular dystrophy type 1D
17
18 (MDC1D) OMIM 608840). Whilst the precise pathway in which these proteins function is
19
20 unclear, recent work suggests that SGK196 is a glycosylation specific O-mannose kinase and that
21
22 FKR, FKTN, TMEM5, B3GNT1 and LARGE all contribute to the generation of an extracellular matrix
23
24 binding moiety on the resulting phosphorylated core M3 glycan (38). The loss of matrix binding is
25
26 associated with a profound reduction in the binding of either I1H6 and/or VIA4-1 antibodies to α -
27
28 dystroglycan (40). In addition a deficiency of Dol-P-Man synthase subunit DPM2 and DPM3
29
30 indicates a possible link between the congenital disorders of glycosylation and the
31
32 dystroglycanopathies. However, it is mutations in FKR that underlie LGMD2I, which is one of
33
34 the most frequent autosomal recessive forms of LGMD (Limb girdle muscular dystrophy) in the
35
36 UK, reported to make up 19.1% of the total LGMD group, with a prevalence of 0.43/100 000 .
37
38
39
40
41
42
43
44
45
46

47 We previously generated a mouse model for FKR related disease by inducing a knock-down in
48
49 *Fkrp* expression via the insertion of a floxed Neomycin cassette into intron 2 of the mouse *Fkrp*
50
51 gene (*FKRP*^{KD}). This resulted in perinatal lethality due to central nervous system involvement
52
53 and whilst this model has proved useful in studies of disease pathogenesis, it is limited in regard
54
55 to its potential for evaluating potential therapies aimed at restoring muscle function. In order to
56
57
58
59
60

1
2
3 overcome this we have now crossed the FKRP^{KD} line of mice with one expressing *Cre*
4 *recombinase* under the control of the Sox1 (Sex determining region Y-box 1) promoter, and
5
6
7
8 show here that this strategy successfully restored Fkrp activity in the brain but not muscle. This
9
10 new line, henceforth referred to as FKRP_{MD}, lives a normal lifespan and begins to show muscle
11
12 damage at around 6 weeks of age and develops a progressive muscular dystrophy by 12 weeks,
13
14
15 thereby representing a new mouse model of the less severe end of the dystroglycanopathy
16
17
18 spectrum.
19

20
21
22
23
24 Whilst there have been two recent reports of the successful restoration of functional
25
26 glycosylation and amelioration of the muscle pathology by AAV (Adeno-Associated Virus)
27
28 vectors carrying either FKRP (41) or fukutin (42), one of the most promising forms of therapy
29
30 proposed in recent years for the dystroglycanopathies is the up-regulation of LARGE; a
31
32 bifunctional glycosyltransferase that alternately transfers xylose and glucuronic acid to generate
33
34 a heteropolysaccharide that confers α -dystroglycan with its ligand binding properties (43). This
35
36 is based on observations showing that LARGE is able to restore α -dystroglycan glycosylation
37
38 and functional laminin binding to cells taken from patients with congenital muscular dystrophy
39
40 (FCMD, MEB and WWS), seemingly irrespective of the gene involved (44). Whilst this
41
42
43 response may be dependent on the availability of O-mannosyl phosphate acceptor sites (32), this
44
45 strategy is still considered as being potentially useful for a wide range of patients. We have
46
47
48 previously shown that in mice, over-expression of LARGE on a wild type background induces
49
50
51 no overt pathology and is only associated with a minor loss of force in response to eccentric
52
53
54 exercise in older mice, supporting the idea that increasing levels of this glycosyltransferase may
55
56
57 represent an important therapeutic approach (45). However, it remains crucial to test such a
58
59
60

1
2
3 strategy on a disease background and in order to do this we crossed our newly generated
4
5 FKRP_{MD} mouse line with one of the original *LARGE* overexpressing lines (45). Somewhat
6
7
8 surprisingly we report that this fails to ameliorate the phenotype and in a proportion of mice
9
10 leads to a worsening of the disease process despite a marked increase in dystroglycan
11
12 glycosylation implying that any future strategies based upon *LARGE* up-regulation require
13
14 careful management.
15
16
17
18
19
20
21

22 Results

23 24 Restoration of *Fkrp* levels in the central nervous system prevents the perinatal lethality of 25 26 FKRP^{KD} mice. 27 28 29

30 FKRP^{KD} mice have a significant reduction in *Fkrp* expression in the muscle and brain, compared
31
32 to wild type mice, which we attributed to the insertion of the floxed Neomycin cassette into
33
34 intron 2 (46). Since we believed that central nervous system involvement was responsible for the
35
36 perinatal mortality, we set out to restore *Fkrp* expression in the central nervous system by
37
38 crossing the FKRP^{KD} line with one expressing Cre recombinase under the Sox1 promoter.
39
40 FKRP^{KD} mice expressing the Sox1 Cre transgene are henceforth referred to as FKRP_{MD}. This
41
42 cross should delete the neomycin cassette from exon 2 in neuroectoderm derived tissues. Since
43
44 defects in the pial basement membrane due to a loss of α -dystroglycan are thought to be central
45
46 to the brain phenotype of FKRP^{KD} mice (46,47) we examined paraffin wax embedded coronal
47
48 sections of the cortex of newborn mice. These sections showed a clear disruption of cortical
49
50 architecture in the FKRP^{KD} (Figure 1B) but no overt abnormalities in the FKRP_{MD} mice, the
51
52 latter of which were comparable to wild type (Figure 1A and C). IIH6 immunolabelling at the
53
54
55
56
57
58
59
60

1
2
3 pial basement membrane of the FKRP_{MD} was comparable to that of WT (Figure 1A and C) but
4
5 not the FKRP^{KD} (Figure 1B) and immunolabelling of frozen sections with a pan laminin antibody
6
7 showed that the disorganisation of the pial basement membrane apparent in FKRP^{KD} mice
8
9 (Figure 1E) had been restored to that of WT in the FKRP_{MD} (Figure 1D and F). In order to
10
11 further confirm that this strategy was successful we undertook an analysis of muscle and brain
12
13 tissue from the FKRP_{MD} mice using quantitative RT PCR. This showed that whilst a marked
14
15 reduction in *Fkrp* transcript levels was still apparent in the muscle of FKRP_{MD} mice, levels had
16
17 been restored to that of wild type in the brain (Figure 1G). We previously showed that the
18
19 percentage knock-down of *Fkrp* in the FKRP^{KD} mouse was similar in all tissues. Here we show
20
21 that the percentage knock-down of *Fkrp* in the muscle of the FKRP_{MD} was similar to that seen in
22
23 the brain of the FKRP^{KD} at E15.5 (Figure 1H).
24
25
26
27
28
29
30
31
32

33 **Reduced *Fkrp* levels in skeletal muscle are associated with a progressive muscular**
34 **dystrophy.**
35

36
37
38 FKRP_{MD} male mice were shown to have a 12 and 20 week body weight not significantly
39
40 different from control mice although female body weight was reduced at 20 but not 12 weeks
41
42 relative to controls (Figure 2A). The lifespan and general behaviour of FKRP_{MD} mice was
43
44 indistinguishable from their wild type littermates.
45
46
47
48

49 Haematoxylin and eosin stained sections of newborn FKRP_{MD} muscle showed no evidence of
50
51 muscle fibre necrosis either in the fore or hindlimb muscles (data not shown). However, by 6
52
53 weeks of age occasional areas of small basophilic regenerating fibres and inflammatory
54
55 infiltrates could be seen in the FKRP_{MD} gastrocnemius (Figure 2C). This feature was quite
56
57
58
59
60

1
2
3 variable between individuals with some mice showing only minimal evidence of any pathology
4
5 at this age. By 12 weeks of age both the gastrocnemius (Figure 2E) and the diaphragm (data not
6
7 shown) of all FKRP_{MD} mice exhibited fibre degeneration characterised by sarcoplasmic
8
9 hyalinisation, loss of cross striations, and sarcoplasmic fragmentation and frequent groups of
10
11 small, regenerative myofibres, with large, centralised nuclei and a granular pale basophilic
12
13 cytoplasm (Figure 2 E). Small infiltrates of macrophages, lymphocytes and rare plasma cells,
14
15 were observed to invade the interstitium and infiltrate necrotic myofibres. At 30 weeks there was
16
17 evidence of an attenuation of muscle fibre degeneration and regeneration with clusters of
18
19 basophilic regenerative fibres being only occasionally evident together with rare, interstitial
20
21 lymphoplasmacytic foci. Representative images of the diaphragm, gastrocnemius and
22
23 quadriceps at 30 weeks are shown in Figure 2 G - K.
24
25
26
27
28
29

30 Interestingly, the soleus of the FKRP_{MD} showed evidence of only minimal damage even at 30
31
32 weeks of age, reflected by the low percentage of central nucleation which is a marker of previous
33
34 rounds of degeneration and regeneration (Figure 2 L-M). This parameter nonetheless increased
35
36 between 12 and 30 weeks of age in all three muscles (gastrocnemius (48.9% to 57.3%), soleus
37
38 (5.6% to 20.9%) and diaphragm (32.4% to 40.7%), with a Generalised Estimating Equations
39
40 model showing that age, muscle and genotype were significant interacting factors affecting the
41
42 percentage of centrally nucleated muscle fibres (Figure 2 L-M). In contrast to previous findings
43
44 in the dystrophin deficient *mdx* mouse, the diaphragm did not seem to be more severely affected
45
46 than the limb muscles. Muscle sampled from wild type littermates at either 12 or 30 week time
47
48 points was histologically unremarkable, exhibiting normal histopathological changes for mice of
49
50 this genetic background i.e. the presence of minimal, rare, interstitial, lymphoplasmacytic
51
52 infiltrates.
53
54
55
56
57
58
59
60

1
2
3
4
5
6
7 **A reduction in α -dystroglycan glycosylation is associated with an alteration in laminin α 2**
8
9 **and α 4 expression.**

10
11
12 The skeletal muscle of the FKRP_{MD} mice displayed a near absence of immunolabelling with the
13
14 IIH6 antibody relative to wild type littermates at 30 weeks of age (Figure 6B), with Western
15
16 blotting further confirming the absence of functional glycosylation as judged by the absence of
17
18 the IIH6 epitope and also showed that β -dystroglycan was unchanged (Figure 3G).
19
20 Immunolabelling for laminin α 2 which has previously been shown to be variably reduced in
21
22 cases of LGMD2I (48), was shown to be increased on some fibres but decreased on others
23
24 relative to WT controls in the FKRP_{MD} at 12 weeks. Those fibres with a higher level tended to be
25
26 associated with areas of increased cellular activity, whilst larger fibres showed either a slight
27
28 decrease or similar levels to that of WT controls (Figure 3A-F). The application of a look up
29
30 table to these images shows this variation more clearly (Figure 3H,I).
31
32
33
34
35

36
37 Laminin α 4 has previously been shown to be up-regulated in the basement membranes of blood
38
39 vessels, the perineurium of intramuscular nerves, and isolated regenerating muscle fibres of
40
41 laminin α 2 deficient mice (*dy/dy*) (49). In wild type controls laminin α 4 localised to the
42
43 capillaries, nerves and neuromuscular junctions (Figure 4A,C,D), however in the FKRP_{MD} at 12
44
45 weeks of age laminin α 4 was additionally increased at the sarcolemma of small groups of fibres.
46
47 By 30 weeks of age a higher proportion of fibres showed laminin α 4 at the sarcolemma than at
48
49 earlier ages (Figure 4D,F). This was the case for each of the muscles examined (diaphragm,
50
51 quadriceps and triceps). This up-regulation was not specifically associated with regenerating
52
53
54
55
56
57
58
59
60

1
2
3 fibres as determined by immunolabelling with developmental myosin which only labelled very
4
5 few fibres at either 12 or 30 weeks.
6
7
8
9

10
11
12 **The overexpression of LARGE leads to a shortened lifespan and worsening of the FKRP_{MD}**
13 **phenotype.**
14
15

16
17
18 Previous work indicated that the upregulation of LARGE could be beneficial in the
19
20 dystroglycanopathies (44,50,51). Contrary to expectation FKRP_{MD} overexpressing LARGE
21
22 (FKRP_{MD}LARGE) had a reduced lifespan in contrast to FKRP_{MD} mice - a subsequent
23
24 deterioration in the overall condition of FKRP_{MD}LARGE mice led to some mice being culled at a
25
26 humane end point which was often around 27 weeks of age. FKRP_{MD}LARGE displayed normal
27
28 behaviour, aside from an abnormal stance and a partial collapse of the leg extensor reflex, a
29
30 feature not observed in the FKRP_{MD} mice.
31
32
33

34
35 In keeping with the more severe phenotype, FKRP_{MD}LARGE mice displayed a more severe
36
37 pathology than age-matched FKRP_{MD} controls at 12 weeks as indicated by a marked variation in
38
39 fibre size, centrally nucleated muscle fibres (Supplementary Figure 1) and significant increases
40
41 in the number of split fibres (Figure 7D). A Generalised Estimating Equations statistical model
42
43 showed that age, genotype and muscle were significant factors affecting the percentage of
44
45 centrally nucleated fibres suggesting that LARGE upregulation significantly increased the
46
47 percentage of centrally nucleated fibres at both 12 and 30 weeks of age, relative to the FKRP_{MD}
48
49 (Figure 7). There was in addition a more pronounced expansion of the interstitium with small to
50
51 moderate amounts of variably-mature fibroadipose tissue and a substantial inflammatory
52
53 component, which infiltrated both the interstitium and necrotic muscle fibres and was comprised
54
55
56
57
58
59
60

1
2
3 of moderate numbers of neutrophils, macrophages and lesser numbers of lymphocytes and
4 plasma cells (Supplementary Figure 1). This was seen in all muscles examined at 12 weeks of
5 age, including the diaphragm, gastrocnemius, tibialis anterior (TA) and soleus (Supplementary
6 Figure 1).
7
8
9
10
11
12
13
14
15
16

17 In those mice that survived to 30 weeks there was a noticeable hypertrophy of many fibres,
18 (relative to the FKRP_{MD}). Individual (predominantly centrally nucleated) muscle fibres were
19 occasionally surrounded by moderate to large amounts of compact, fibrous connective tissue and
20 infiltrates of fat (Figure 5B, D, F, H), with some muscle fibres mineralised. At this later time
21 point as in the FKRP_{MD}, there was minimal degeneration and necrosis although the inflammatory
22 infiltration was more marked with infiltration by both neutrophils and macrophages in the
23 diaphragm and gastrocnemius. Alizarin red staining showed a marked increase in the presence of
24 large calcium deposits in the FKRP_{MD}LARGE relative to the FKRP_{MD} mice (Figure 5 I-K). This
25 was the case for all the muscles examined including the soleus. Alizarin red staining was also
26 markedly worse in the diaphragm of the FKRP_{MD}LARGE mice, relative to the gastrocnemius at
27 12 weeks of age, a difference between these muscles that was not evident in the FKRP_{MD} mice at
28 this age.
29
30
31
32
33
34
35
36
37
38
39
40
41
42
43
44
45
46
47
48

49 **FKRP_{MD}LARGE mice display an increase in IIIH6 labelling and laminin deposition.**

50
51
52 The glycosylation of α -DG as assessed by IIIH6 immunolabelling was increased in all
53 FKRP_{MD}LARGE muscles examined (diaphragm, gastrocnemius and soleus) relative to wild type
54 mice (Figure 6 shows the gastrocnemius), and levels were comparable to that of the original
55
56
57
58
59
60

1
2
3 LARGE transgenic line (data not shown). Laminin $\alpha 2$ deposition at the basement membrane was
4 increased in FKRP_{MD}LARGE mice relative to FKRP_{MD} mice or wild type. Whilst regenerating
5 fibres are known to express higher levels of basement membrane proteins, this increase extended
6 beyond the clusters of small regenerating fibres. The number of fibres with sarcolemmal
7 labelling for laminin $\alpha 4$ was also increased in the FKRP_{MD}LARGE mice relative to FKRP_{MD}
8 mice (Figure 6). Western blot analysis of muscle at 15-20 weeks showed that transgene
9 expression in either the wild type or FKRP_{MD} gives rise to an increase in laminin binding relative
10 to wild type confirming that expression of the transgene led to the hyperglycosylation of α -DG.
11 (Figure 7).
12
13
14
15
16
17
18
19
20
21
22
23
24
25
26
27
28

29 **FKRP_{MD}LARGE mice show a physiological deficit relative to the FKRP_{MD}.**

30
31
32 To compare the functional properties associated with a knock-down of Fkrp and how this was
33 altered by the transgenic expression of LARGE we subjected the TA muscles of anaesthetized
34 mice to a protocol of 10 eccentric (lengthening) contractions *in situ*. The protocol induced a 15%
35 stretch during each of 10 maximal isometric contractions stimulated 2 minutes apart. Isometric
36 tetanic force was measured prior to each stretch and expressed as a percentage of baseline
37 isometric force. FKRP_{MD} mice showed a similar resistance to eccentric contraction-induced
38 injury to non-transgenic age-matched wild type controls (101.1% and 118.5% of baseline
39 isometric force generated in the last contraction respectively) with only a small significant drop
40 in force after contraction 10. However, FKRP_{MD}LARGE showed a significant reduction in their
41 resistance (72.5% of baseline isometric force in the last contraction) relative to controls (118.1%
42 of baseline isometric force in the last contraction) confirming that the worsened phenotype
43
44
45
46
47
48
49
50
51
52
53
54
55
56
57
58
59
60

1
2
3 evident on histological analysis had translated into a measurable physiological deficit (Figure 8).
4
5
6 No significant differences were observed for the force-frequency relationship between any of the
7
8 genotypes (data not shown).
9
10
11
12
13
14
15
16
17
18
19
20
21
22
23
24
25
26
27
28
29
30
31
32
33
34
35
36
37
38
39
40
41
42
43
44
45
46
47
48
49
50
51
52
53
54
55
56
57
58
59
60

For Peer Review

Discussion.

LGMD2I is one of the most frequent autosomal recessive forms of LGMD and in the UK has been reported to make up 19.1% of the total LGMD group with a prevalence of 0.43/100 000 (52,53). Whilst the spectrum of disease in the dystroglycanopathies is wide, a significant proportion of patients are affected by relatively mild limb girdle muscular dystrophies without any central nervous system involvement, making it a good target for developing therapies. In order to gain insight into the disease pathogenesis of FKRP associated muscular dystrophy we previously generated a mouse model with a knock-down in *Fkrp* (FKRP^{KD}) that displayed a muscle eye brain phenotype. Whilst this model provided insight into the eye and brain phenotype (46), it died around the time of birth due to the severity of central nervous system involvement (47) and so was less useful for investigating the consequences of a reduction in *Fkrp* on postnatal muscle growth and function and for evaluating therapeutic strategies aimed at ameliorating the skeletal muscle phenotype.

In mammals, the cortex develops in an “inside out” manner, with migration of post mitotic neurons from the proliferative neuroepithelium (ventricular zone) to the cortical plate with each layer of post-mitotic neurons forming a more superficial layer than the last (54). The majority of neuronal migration is radial and is mediated by a scaffold of radial glial cells which extend from the ventricular zone (where their cell bodies are located) to the pial basement membrane. In the present report we addressed the perinatal lethality of the FKRP^{KD} mouse by crossing it with a transgenic line in which Cre recombinase is expressed under control of the Sox-1 promoter to generate $\text{FKRP}^{\text{KD}}/\text{Sox1Cre}$ mice which we refer to as FKRP_{MD} . The Sox1 promoter is known to drive expression in the neuroectoderm early during development (55) and this cross resulted in mice with wild type *Fkrp* transcript levels in the brain, a restoration of IIH6 immunolabelling at

1
2
3 the pial basement membrane and normal cortical architecture. Previous work has indicated that
4 the restoration of glial rather than neuronal dystroglycan that plays a crucial role in forebrain
5 development (56) and the restoration of the pial basement membrane and cortical organisation
6 we observed was therefore consistent with these observations. As expected there remained an
7 approximate 80% reduction of *Fkrp* transcript levels in the skeletal muscle which was associated
8 with the loss of the laminin binding epitope IIH6 as previously reported for the FKRP^{KD} line
9 (21).
10
11
12
13
14
15
16
17
18
19

20
21 Despite the absence of the laminin binding IIH6 epitope from birth, the onset of muscle
22 degeneration first occurred around 6 weeks of age in the majority of animals and by 12 weeks of
23 age a marked pathology was evident in all FKRP_{MD} mice. Western blot analysis confirmed that
24 the IIH6 epitope was completely absent. This also resulted in the loss of laminin binding which
25 is consistent with previous studies in the LARGE_{myd}, POMGnT_{null} and POMT1 mice that also
26 report a reduction in the ability to bind laminin and develop a severe muscular dystrophy (57).
27
28 In contrast, the muscle of a mouse model of FCMD (FCMD Hp⁻) which contains a
29 retrotransposal insertion in the mouse fukutin ortholog also failed to label with IIH6 but retained
30 the ability to bind laminin albeit at 50% of the levels of controls. This mouse did not display any
31 signs of a muscular dystrophy suggesting the existence of a threshold of glycosylation/laminin
32 binding activity which was met in the FCMD mice (58) but not in the LARGE_{myd} and
33 POMGnT_{null} or our FKRP_{MD} mice.
34
35
36
37
38
39
40
41
42
43
44
45
46
47
48
49

50 All laminin isoforms with LN (Laminin N-terminal) domains play an integral role in basement
51 membrane assembly by anchoring to cell surfaces, self polymerizing, and binding to nidogen and
52 collagen IV (1). Laminin 211 is the major laminin isoform present in skeletal muscle and is
53 reduced albeit not invariably in the skeletal muscle of dystroglycanopathy patients. A variation in
54
55
56
57
58
59
60

1
2
3 laminin $\alpha 2$ immunolabelling was also observed in FKRP_{MD} mice at 12 weeks with higher levels
4
5 of labelling apparent on small regenerating fibres whilst the majority of larger fibres either
6
7 showed similar levels to that of controls or a reduction implying that a reduction in glycosylation
8
9 may influence the turnover and/or stability of laminin 211 in the basement membrane of mature
10
11 muscle fibres. Interestingly, there was no obvious reduction in perlecan in the FKRP_{MD} mice
12
13 when compared to wildtype mice (data not shown) despite previous reports of a reduction in the
14
15 perlecan-binding activity and its mis-localisation in the brains of Large_{myd} and dystroglycan null
16
17 mice (59). However, it may be that laminin $\alpha 2$ rather than perlecan is the main binding partner
18
19 for α -dystroglycan in muscle, indeed the binding properties of α -dystroglycan are known to be
20
21 different in brain and muscle (60).
22
23
24
25
26

27
28 We observed a redistribution of laminin $\alpha 4$ in the FKRP_{MD} muscle which has also been reported
29
30 in laminin $\alpha 2$ deficient mice (49). Laminin $\alpha 4$ normally locates to the basement membranes of
31
32 blood vessels, the endoneurium of the intramuscular nerves, and the neuromuscular junction in
33
34 neonatal skeletal muscle (49). In adult muscle it locates to the perineurium of adult peripheral
35
36 nerve. Laminin $\alpha 4$ lacks the ability to self-polymerise (61) due to the absence of the N-terminal
37
38 domain, and consequently has the potential to interfere with basal lamina formation where
39
40 laminin $\alpha 2$ is a major component. It also displays a low affinity binding for α -dystroglycan,
41
42 sulfatides, and integrins $\alpha 6\beta 1$ and $\alpha 7\beta 1$ (62), properties that suggest it may be an ineffective
43
44 substitute for laminin $\alpha 2$. However, the up-regulation of laminin $\alpha 4$, which is also a feature of
45
46 laminin $\alpha 2$ deficiency may nonetheless be of functional significance since recent work in the
47
48 zebra fish suggests that its up-regulation in damaged fibres contributes to fibre survival (63).
49
50
51
52
53
54 Interestingly, an increase in the number of fibres with laminin $\alpha 4$ at the sarcolemma was
55
56
57
58
59
60

1
2
3 observed to increase with age in the FKRP_{MD}, implying that a similar scenario may apply to our
4
5 mice.
6
7

8
9 LARGE is a bifunctional glycosyltransferase thought to be essential for conferring α -
10
11 dystroglycan with the ability to bind laminin. The over-expression of LARGE has been shown to
12
13 increase-DG glycosylation in both wild type and cells from dystroglycanopathy patients,
14
15 irrespective of their primary gene defect (44). Whilst more recent work now demonstrates that
16
17 the ability of LARGE to hyperglycosylate α -dystroglycan is dependent on the availability of O-
18
19 mannosyl phosphate acceptor sites and correlates with the severity of the clinical phenotype (32);
20
21 this strategy is still considered as being potentially useful for a wide range of patients.
22
23 Furthermore, the viral delivery of LARGE to skeletal muscle in animal models of
24
25 dystroglycanopathy has been reported to have identical effects *in vivo*, suggesting that the
26
27 restoration of functional glycosylation may be a valuable therapeutic approach in this group of
28
29 disorders (44,58). We previously generated a number of transgenic lines overexpressing LARGE
30
31 (45) and have now crossed one of these lines with our FKRP_{MD} mice. On a wild type
32
33 background the up-regulation of LARGE is not associated with any muscle fibre degeneration
34
35 but there is a mild loss of force upon eccentric exercise in the TA of older animals (45),
36
37 suggesting some form of subtle abnormality in basement membrane turnover occurs over an
38
39 extended time period (64). However, when we crossed the FKRP_{MD} line with the LARGE
40
41 transgenic the pathology of the FKRP_{MD} phenotype worsened with an increased percentage of
42
43 centrally nucleated fibres in all the muscles examined relative to the FKRP_{MD}. Additional
44
45 features such as calcium deposits, evidence of fibrosis and replacement of muscle fibres by
46
47 adipocytes were also more evident in the presence of the LARGE transgene and the soleus
48
49 muscle which was largely spared in the FKRP_{MD} showed clear evidence of pathology in the
50
51
52
53
54
55
56
57
58
59
60

1
2
3 presence of the LARGE transgene. The promoter driving the LARGE transgene expresses at
4 equivalent levels in both slow and fast fibres therefore these observations reflect a differential
5
6 pattern of muscle involvement in the FKRP_{MD}.
7
8
9

10
11 Whilst there are several differences between our study and those which previously indicated that
12 the up-regulation of LARGE would be beneficial such as the method of gene delivery, promoter
13 used to drive expression, and animal model, the most significant difference relates to the timing
14 over which LARGE was overexpressed, and the duration of the period of observation. For
15 example, LARGE was introduced into the Large^{myd}, POMGnT1^{-/-} and FCMD Hp⁻ mice via AAV
16 vectors at postnatal data 2-4 and then evaluated 4 weeks later (44,58). More recently Yu et al
17 (50) injected AAV9-LARGE (expression driven by the β -actin promoter) via into the newborn
18 heart and adult tail vein of POMGnT1null and LARGE_{myd} mice and looked at expression at 2
19 months (newborn injections) and 1 month (adult tail vein injections) later. These authors noted
20 significant improvement of the histological appearance of the muscle and amelioration of the
21 phenotype. Barresi et al (44) also administered *LARGE* to older Large^{myd} mice, aged between 12
22 days and 5 weeks but reported that this was associated with muscle inflammation and a loss of
23 IIH6 immunolabelling (*LARGE* up-regulation) as the mice aged.
24
25
26
27
28
29
30
31
32
33
34
35
36
37
38
39
40
41
42

43 These findings are in marked contrast to those of our own using transgenesis and would seem to
44 imply that the time period over which LARGE is up-regulated and/or the stage of development
45 that it is initiated determine the outcome. Here we have shown that despite the restoration of
46 laminin binding in the FKRP_{MD}LARGE there was a significant loss of force in response to
47 eccentric exercise which was not seen in the FKRP_{MD} confirming that the overexpression of
48 LARGE had worsened the phenotype as indicated by the histological analyses. The reasons for
49 this remain unclear however, it is possible that on a disease background, specifically one in
50
51
52
53
54
55
56
57
58
59
60

1
2
3 which the glycosylation of α -dystroglycan is reduced or absent, LARGE not only targets
4
5 additional proteins, the hyperglycosylation of which is detrimental to muscle, but may also lead
6
7 to a functionally relevant alteration in the glycosylation pattern of α -DG itself. In support of
8
9 these two concepts it has previously been shown that LARGE over-expression in α -DG-deficient
10
11 cells leads to the expression of the I1H6 epitope (65) and that LARGE acts not only on the O-
12
13 mannose glycans but also complex N-glycans and mucin O-GalNAc (N-Acetylgalactosamine)
14
15 glycans of α -DG (66). Previous work in ES (Embryonic Stem) cells indicates that neither
16
17 integrin nor dystroglycan are individually required for assembly of the basement membrane but
18
19 they do regulate both their own expression and that of other basement membrane components
20
21 (67). It is therefore possible that this system of regulation is perturbed by an altered pattern of α -
22
23 dystroglycan glycosylation, perhaps by compromising the turnover process of the basement
24
25 membrane. Finally it should also be noted that as a consequence of the transgenic approach
26
27 adopted here, the FKRP_{MD}LARGE mice are on a different background to the FKRP_{MD} mouse.
28
29 However, we consider this an unlikely cause of the worsened phenotype since histological
30
31 evaluation of wildtype *LARGE* overexpressing mice on this new genetic background failed to
32
33 identify any evidence of a dystrophic pathology.

34
35
36
37
38
39
40
41
42 Our work reports the first transgenic up-regulation of LARGE on a disease background. Whilst
43
44 the onset of disease in the FKRP_{MD}LARGE mice was not markedly different to the FKRP_{MD},
45
46 suggesting that the over-expression of LARGE did not adversely affect the early stages of
47
48 muscle development, several aspects of the disease process were significantly worse. The
49
50 reasons for this are unclear at the present time, but emphasise the value of determining the effect
51
52 of overexpression on a disease background over an extended period and suggest that any
53
54 therapeutic approach involving LARGE up-regulation requires careful management.
55
56
57
58
59
60

Materials and Methods.

Generation of FKRP-Neo^{Tyr307Asn+/+Sox1Cre} mice (FKRP_{MD})

All animal experiments were carried out under license from the Home Office (UK) in accordance with The Animals (Scientific Procedures) Act 1986 and were approved by Royal Veterinary College ethical committee. The FKRP-Neo^{Tyr307Asn+/+} (FKRP^{KD}) mouse colony (47) was crossed with a second transgenic line expressing *Cre recombinase* throughout the developing neural tube under the Sox1 promoter (a kind gift from Professor Liz Robertson, Sir William Dunn School of Pathology, Oxford U.K.) (68). Briefly FKRP-Neo^{Tyr307Asn+/-} were crossed with Sox1Cre mice and the resulting FKRP-Neo^{Tyr307Asn+/-Sox1Cre} mice were bred with FKRP-Neo^{Tyr307Asn+/-} mice which generated FKRP-Neo^{Tyr307Asn+/+Sox1Cre} mice, referred to as FKRP_{MD}. Thus, the first cross introduced the Sox1Cre transgene into the background of the FKRP^{KD} colony, while the second first generation cross generated the FKRP_{MD} offspring at a frequency of approximately 7%. FKRP_{MD} mice are fertile and breeding them with FKRP-Neo^{Tyr307Asn+/-} mice increased the incidence of mice to approximately 14%. However, pairing two FKRP-Neo^{Tyr307Asn+/-Sox1Cre} heterozygote mice resulted in high pre-weaning losses, with a number of offspring suffering from hydrocephalus.

Generation of FKRP-Neo^{Tyr307Asn+/+Sox1CreLARGE} (FKRP_{MD}LARGE).

The following strategy was used to generate FKRP_{MD}, FKRP^{KD} and FKRP_{MD} LARGE mice. FKRP-Neo^{Tyr307Asn+/-Sox1Cre} mice were crossed with a transgenic mouse line (LV5) overexpressing human LARGE (45) to introduce the LARGE transgene into the background of the FKRP_{MD}

1
2
3 mice. FKRP-Neo^{Tyr307Asn+/-Sox1CreLARGE} mice were then crossed with FKRP-Neo^{Tyr307Asn+/-} to
4
5 generate FKRP-Neo^{Tyr307Asn+/+Sox1CreLARGE} mice, henceforth referred to as FKRP_{MD}LARGE mice.
6
7
8
9
10

11 *Genotyping FKRP_{MD} offspring*

12
13
14
15 Offspring were genotyped by PCR analysis using either ear or tail biopsies. Genomic DNA from
16 the mouse tissue was prepared by digestion in Direct PCR Lysis Ear or Tail buffer (Eurogentec)
17 respectively containing 0.2mg/mL Proteinase K (Roche Diagnostics) at 55°C overnight. The
18 Proteinase K was heat inactivated at 85°C for 30 minutes and PCR was performed with the crude
19 DNA lysate using Biomix Red PCR Kit (Bioline) with the following multiplex primers for Fkrp
20 (FKRP-F: CTAGGAGGTTGAGGATGATGG, FKRP-R: GTTGTGCTTAAACCACCTTC, and
21 FKRP-NeoF:GGTGGATTAGATAAATGC), Cre recombinase (Cre-F:
22 CCCAGGCTAAGTGCCTTCTC and Cre-R: CCAGGTTTCGTTCACTCATGG) and *LARGE*
23 (Large-F:TAATACGACTCACTATAGGG Large-R: AAGGTTCTCGCTGTCTCC).
24
25
26
27
28
29
30
31
32
33
34
35
36
37
38
39
40

41 *Histology and Immunocytochemistry*

42
43
44 For standard histochemistry, newborn mice were collected and fixed in Bouins (Sigma) and
45 transferred to 70% ethanol prior to processing and embedding in paraffin wax. Samples were
46 serially sectioned at 5µm, with sections collected onto charged slides (Superfrost Plus, VWR),
47 rehydrated and stained with haematoxylin and eosin, using standard methods. For
48 immunohistochemistry sections were deparaffinised and rehydrated prior to incubation with anti
49 α-dystroglycan (IIH6, Millipore) diluted in phosphate buffered saline containing 0.05% tween 20
50
51
52
53
54
55
56
57
58
59
60

1
2
3 (Sigma) for 1 hour at room temperature. Visualisation of the I1H6 was performed using the
4
5 Envision system (DAKO).
6
7
8
9

10
11
12 Alternatively, muscle and brain samples were frozen in isopentane cooled in liquid nitrogen and
13
14 10µm sections were cut using a Bright Cryostat. These were then stained with haematoxylin and
15
16 eosin using standard methods to evaluate general tissue pathology and calculate the percentage
17
18 of centrally located nuclei. Additionally, Alizarin Red staining was performed to identify
19
20 calcium deposits. Images of newborn mouse heads and muscles stained with these histochemical
21
22 methods were digitally captured using a DM4000B upright microscope (Leica, Germany)
23
24 interfaced with a DC500 colour camera (Leica) using the Leica Application Suite (Leica
25
26 Microsystems) software provided and compiled into figures using Photoshop CS4 or CS5
27
28 (Adobe, U.S.A.). Figures were compiled using Photoshop CS (Adobe, U.S.A.). All
29
30 observations are based on a minimum of n=3 (of either sex), and representative images are
31
32 shown. Counts of centrally nucleated muscle fibres were made across an entire section from
33
34 each individual mouse muscle (n=3 for wildtype, FKRP_{MD} and FKRP_{MD}LARGE mice at 12 and
35
36 30 weeks of age) randomly chosen from the mid-region of each muscle, with the total number of
37
38 fibres counted numbering approximately 500, 1500 and 2000 muscle fibres in the soleus,
39
40 diaphragm and gastrocnemius respectively. The incidence of split muscle fibres was based on
41
42 counts of approximately 2000 muscle fibres across an entire section from the mid-belly region of
43
44 12 week old wildtype, FKRP_{MD} and FKRP_{MD}LARGE gastrocnemius (n=3 for all genotypes).
45
46
47
48
49
50
51
52
53
54
55
56
57
58
59
60

1
2
3 For immunohistochemical analysis of muscle and brain, cryosections were immunolabelled with
4 rabbit anti pan-laminin (Sigma-Aldrich), rat anti laminin $\alpha 2$ (4H8, Abcam), goat anti-laminin $\alpha 4$
5 (R&D Systems) and the IIH6 antibody against a glycosylated epitope of α -DG (Millipore). This
6 was followed by anti-rat/rabbit/goat tagged with Alexa 488 or 594 (Molecular Probes) for 30
7 minutes, with the exception of IIH6 which was labelled with anti-IgM biotinylated antibody (30
8 minutes) followed by streptavidin conjugated with Alexa 488/594 (30 minutes). Nuclei were
9 stained with Hoechst 33342 (Sigma-Aldrich). All dilutions and washes were made in phosphate
10 buffered saline. Sections were mounted in aqueous mountant and viewed with epifluorescence
11 using a DM4000B upright microscope (Leica, Germany). Images were digitally captured with
12 an Axiovision mRM monochrome camera, (Zeiss, UK) and compiled using Photoshop CS
13 (Adobe, U.S.A.). Where direct comparisons have been made, fluorescent images were captured
14 with equal exposure and have had equal scaling applied. All observations are based on a
15 minimum of n=3 (of either sex), representative images are shown.
16
17
18
19
20
21
22
23
24
25
26
27
28
29
30
31
32
33
34
35
36
37

38 *qRT-PCR analysis.*

39
40
41 Brain and muscle were dissected out and homogenised with liquid nitrogen using a mortar and
42 pestle and the lysate passed through a QiaShredder[®](Qiagen). RNA was isolated from the
43 homogenised tissue using an RNeasy[®]kit (Qiagen) and for muscle RNeasy[®] Fibrous Tissue Kit
44 (Qiagen) eluted with 30 μ l RNase free H₂O. 1 μ g of RNA was reverse transcribed with
45 Superscript[®]III Platinum for qRT-PCR kit (Invitrogen). qRT-PCR was performed on a 7500
46 FAST Real-Time PCR system (Applied Biosystems) using aFAM^(tm) reporter dye system. For
47 each reaction 0.8 μ l of cDNA was used as template in a PCR mix consisting of 1 μ l of primer mix,
48
49
50
51
52
53
54
55
56
57
58
59
60

1
2
3 10 ul TaqMan Universal PCR Mastermix (Applied Biosystems) and 8.2µl H₂O. The primers for
4 the gene expression assays were sourced commercially from Applied Biosystems (*FKRP*
5 Mm00557870_mL, *GAPDH* Mm99999915_gL). Each experiment represents a minimum of n=4
6 (of either sex) and all reactions were performed in triplicate.
7
8
9
10
11
12
13
14
15
16

17 *Western blotting and laminin overlay assay.*

18
19
20 Cell proteins were extracted in sample buffer consisting of 75 mM Tris-HCl, 1% SDS, 2-
21 mercaptoethanol, plus a cocktail of protease inhibitors (Roche). 30µg of soluble proteins were
22 resolved using a NuPage Pre-cast gel (3–8% Tris-acetate; Invitrogen, USA) and then transferred
23 electrophoretically to nitrocellulose membrane (Hybond-PVDF, GE Healthcare, UK.
24 Nitrocellulose strips were blocked in 5% dried non fat milk in phosphate-buffered saline buffer,
25 and then probed with the primary antibodies: anti mouse α -DG I1H6 (Millipore UK,cat,05-593)
26 anti-mouse β -DG (Vector Labs, UK), at room temperature for 1 hour. After washing they were
27 incubated with the appropriate HRP conjugated secondary antibody for one hour: anti-mouse-
28 IgM or anti-mouse-IgG (both from Jackson ImmunoResearch). After washing, membranes were
29 visualized using chemiluminescence (ECL+Plus, GE Healthcare, UK). For the laminin overlay
30 assay, nitrocellulose membranes were blocked for 1 hour in laminin binding buffer (LBB: 10
31 mM triethanolamine, 140 mM NaCl, 1 mM MgCl₂, 1 mM CaCl₂, pH 7.6) containing 5% non-fat
32 dry milk followed by incubation of mouse Engelbreth-Holm-Swarm laminin (Invitrogen,USA)
33 overnight at 4°C in LBB. Membranes were washed and incubated with anti rabbit laminin
34 (Sigma, USA) followed by HRP-anti rabbit IgG (Jackson ImmunoResearch, USA). Blots were
35 visualized using chemiluminescence (ECL+Plus, GE Healthcare,UK).
36
37
38
39
40
41
42
43
44
45
46
47
48
49
50
51
52
53
54
55
56
57
58
59
60

1
2
3
4
5
6
7 *In situ/vivo* muscle electrophysiology.
8

9
10 Mice were surgically prepared as described previously (69,70). Contractions were stimulated in
11 the TA muscle *in situ* via the surgically isolated common peroneal nerve. The TA muscle
12 underwent a series of 5 submaximal isometric contractions as a warm up. Isometric force
13 measurements were made over a range of stimulating frequencies and maximum isometric
14 tetanic force (P_0) was determined from the plateau of the force–frequency curve (20). After
15 completing the final isometric contraction the optimum length (L_0) was measured with digital
16 callipers and the muscle was allowed to rest for 5 min before the eccentric contraction protocol
17 was initiated. A tetanic contraction was induced using a stimulus of 120 Hz (the frequency that
18 resulted in P_0 without causing fatigue during the contraction) for 700 ms. During the last 200 ms
19 of this contraction, the muscle was stretched by 15% of L_0 at a velocity of $0.75 L_0s^{-1}$ and relaxed
20 at $-0.75L_0s^{-1}$. The isometric tension recorded prior to the first stretch was used as a baseline. The
21 muscle was then subjected to 10 eccentric contractions each separated by a 2 min rest period to
22 avoid the confounding effect of muscle fatigue. The isometric tension prior to each stretch was
23 recorded and expressed as a percentage of the baseline tension (69). The mouse was then
24 euthanized and the muscle was carefully removed and weighed.
25
26
27
28
29
30
31
32
33
34
35
36
37
38
39
40
41
42
43
44
45
46
47
48

49 *Statistical analyses.*
50

51
52 Body weights were analysed with a Linear Mixed Effects Model and central nucleation counts
53 were analysed with a General Estimating Equations model, both performed using SPSS Statistics
54 (IBM, U.S.A). The incidence of split fibres was analysed with a one-tailed Mann-Whitney test,
55
56
57
58
59
60

1
2
3 Muscle physiology data were analysed using a Repeated Measures One-way ANOVA with
4
5
6 Tukey's *post-hoc* comparison.
7
8
9

10
11
12 **Acknowledgements:** We would like to acknowledge the kind gift of the Sox1Cre recombinase
13
14 expressing mice from Professor Liz Robertson, Sir William Dunn School of Pathology, Oxford
15
16 U.K and the excellent technical assistance of Alice Nettleton. We also thank Drs. Anne
17
18 Rutkowski and Claudia Mitchell for their helpful discussions during the course of this work. We
19
20 gratefully acknowledge the support of Cure CMD (Congenital Muscular Dystrophy), the
21
22 Muscular Dystrophy Association of America (MDA) and Association Francaise contres les
23
24 Myopathies (AFM). FM is supported by the Great Ormond Street Children's Charity and the
25
26 Biomedical Research Centre and CW is supported by a Medical Research Council studentship.
27
28
29
30
31
32
33
34
35
36
37

38 **Conflict of Interest:** None declared.
39
40
41
42
43
44
45
46
47
48
49
50
51
52
53
54
55
56
57
58
59
60

Reference List

1. Yurchenco,P.D., Patton,B.L. (2009) Developmental and pathogenic mechanisms of basement membrane assembly. *Curr. Pharm. Des*, 15, 1277-1294.
2. Henry,M.D., Williamson,R.A., Campbell,K.P. (1998) Analysis of the role of dystroglycan in early postimplantation mouse development. *Ann. N. Y. Acad. Sci.*, 857, 256-259.
3. Henry,M.D., Campbell,K.P. (1998) A role for dystroglycan in basement membrane assembly. *Cell*, 95, 859-870.
4. Yurchenco,P.D., Amenta,P.S., Patton,B.L. (2004) Basement membrane assembly, stability and activities observed through a developmental lens. *Matrix Biol*, 22, 521-538.
5. Yurchenco,P.D., Cheng,Y.S., Campbell,K., Li,S. (2004) Loss of basement membrane, receptor and cytoskeletal lattices in a laminin-deficient muscular dystrophy. *J Cell Sci*, 117, 735-742.
6. Durbeej,M., Larsson,E., Ibraghimov-Beskrovnaya,O., Roberds,S.L., Campbell,K.P., Ekblom,P. (1995) Non-muscle alpha-dystroglycan is involved in epithelial development. *J. Cell Biol.*, 130, 79-91.
7. Michele,D.E., Barresi,R., Kanagawa,M., Saito,F., Cohn,R.D., Satz,J.S., Dollar,J., Nishino,I., Kelley,R.I., Somer,H., *et al.* (2002) Post-translational disruption of dystroglycan-ligand interactions in congenital muscular dystrophies. *Nature*, 418, 417-422.
8. Ervasti,J.M., Burwell,A.L., Geissler,A.L. (1997) Tissue-specific heterogeneity in alpha-dystroglycan sialoglycosylation. Skeletal muscle alpha-dystroglycan is a latent receptor for Vicia villosa agglutinin b4 masked by sialic acid modification. *J. Biol. Chem.*, 272, 22315-22321.
9. Ervasti,J.M., Campbell,K.P. (1993) A role for the dystrophin-glycoprotein complex as a transmembrane linker between laminin and actin. *J. Cell Biol.*, 122, 809-823.
10. Peng,H.B., Ali,A.A., Daggett,D.F., Rauvala,H., Hassell,J.R., Smalheiser,N.R. (1998) The relationship between perlecan and dystroglycan and its implication in the formation of the neuromuscular junction. *Cell Adhes. Commun.*, 5, 475-489.
11. Bowe,M.A., Deyst,K.A., Leszyk,J.D., Fallon,J.R. (1994) Identification and purification of an agrin receptor from Torpedo postsynaptic membranes: a heteromeric complex related to the dystroglycans. *Neuron*, 12, 1173-1180.

12. Campanelli, J.T., Roberds, S.L., Campbell, K.P., Scheller, R.H. (1994) A role for dystrophin-associated glycoproteins and utrophin in agrin-induced AChR clustering. *Cell*, 77, 663-674.
13. Gee, S.H., Montanaro, F., Lindenbaum, M.H., Carbonetto, S. (1994) Dystroglycan-alpha, a dystrophin-associated glycoprotein, is a functional agrin receptor. *Cell*, 77, 675-686.
14. Sugita, S., Saito, F., Tang, J., Satz, J., Campbell, K., Sudhof, T.C. (2001) A stoichiometric complex of neurexins and dystroglycan in brain. *J. Cell Biol.*, 154, 435-445.
15. Sato, S., Omori, Y., Katoh, K., Kondo, M., Kanagawa, M., Miyata, K., Funabiki, K., Koyasu, T., Kajimura, N., Miyoshi, T., *et al.* (2008) Pikachurin, a dystroglycan ligand, is essential for photoreceptor ribbon synapse formation. *Nat. Neurosci.*, 11, 923-931.
16. Wright, K.M., Lyon, K.A., Leung, H., Leahy, D.J., Ma, L., Ginty, D.D. (2012) Dystroglycan organizes axon guidance cue localization and axonal pathfinding. *Neuron*, 76, 931-944.
17. Hohenester, E., Tisi, D., Talts, J.F., Timpl, R. (1999) The crystal structure of a laminin G-like module reveals the molecular basis of alpha-dystroglycan binding to laminins, perlecan, and agrin. *Mol. Cell*, 4, 783-792.
18. Tisi, D., Talts, J.F., Timpl, R., Hohenester, E. (2000) Structure of the C-terminal laminin G-like domain pair of the laminin alpha2 chain harbouring binding sites for alpha-dystroglycan and heparin. *EMBO J.*, 19, 1432-1440.
19. Michele, D.E., Campbell, K.P. (2003) Dystrophin-glycoprotein complex: post-translational processing and dystroglycan function. *J. Biol. Chem.*, 278, 15457-15460.
20. Yoshida-Moriguchi, T., Yu, L., Stalnakier, S.H., Davis, S., Kunz, S., Madson, M., Oldstone, M.B., Schachter, H., Wells, L., Campbell, K.P. (2010) O-mannosyl phosphorylation of alpha-dystroglycan is required for laminin binding. *Science*, 327, 88-92.
21. Ackroyd, M.R., Skordis, L., Kaluarachchi, M., Godwin, J., Prior, S., Fidanboyly, M., Piercy, R.J., Muntoni, F., Brown, S.C. (2009) Reduced expression of fukutin related protein in mice results in a model for fukutin related protein associated muscular dystrophies. *Brain*, 132, 439-451.
22. Beltran-Valero, D.B., Currier, S., Steinbrecher, A., Celli, J., van Beusekom, E., van der, Z.B., Kayserili, H., Merlini, L., Chitayat, D., Dobyns, W.B., *et al.* (2002) Mutations in the O-mannosyltransferase gene POMT1 give rise to the severe neuronal migration disorder Walker-Warburg syndrome. *Am. J. Hum. Genet.*, 71, 1033-1043.

23. van Reeuwijk J., Janssen,M., van den,E.C., Beltran-Valero de,B.D., Sabatelli,P., Merlini,L., Boon,M., Scheffer,H., Brockington,M., Muntoni,F., *et al.* (2005) POMT2 mutations cause alpha-dystroglycan hypoglycosylation and Walker-Warburg syndrome. *J. Med. Genet.*, 42, 907-912.
24. Yoshida,A., Kobayashi,K., Manya,H., Taniguchi,K., Kano,H., Mizuno,M., Inazu,T., Mitsuhashi,H., Takahashi,S., Takeuchi,M., *et al.* (2001) Muscular dystrophy and neuronal migration disorder caused by mutations in a glycosyltransferase, POMGnT1. *Dev. Cell*, 1, 717-724.
25. Longman,C., Brockington,M., Torelli,S., Jimenez-Mallebrera,C., Kennedy,C., Khalil,N., Feng,L., Saran,R.K., Voit,T., Merlini,L., *et al.* (2003) Mutations in the human LARGE gene cause MDC1D, a novel form of congenital muscular dystrophy with severe mental retardation and abnormal glycosylation of alpha-dystroglycan. *Hum. Mol. Genet.*, 12, 2853-2861.
26. van Reeuwijk J., Grewal,P.K., Salih,M.A., Beltran-Valero de,B.D., McLaughlan,J.M., Michielse,C.B., Herrmann,R., Hewitt,J.E., Steinbrecher,A., Seidahmed,M.Z., *et al.* (2007) Intragenic deletion in the LARGE gene causes Walker-Warburg syndrome. *Hum Genet*, 121, 685-690.
27. Grewal,P.K., Hewitt,J.E. (2002) Mutation of Large, which encodes a putative glycosyltransferase, in an animal model of muscular dystrophy. *Biochim. Biophys. Acta*, 1573, 216-224.
28. Toda,T. (1999) [Fukutin, a novel protein product responsible for Fukuyama-type congenital muscular dystrophy]. *Seikagaku*, 71, 55-61.
29. Brockington,M., Blake,D.J., Prandini,P., Brown,S.C., Torelli,S., Benson,M.A., Ponting,C.P., Estournet,B., Romero,N.B., Mercuri,E., *et al.* (2001) Mutations in the fukutin-related protein gene (FKRP) cause a form of congenital muscular dystrophy with secondary laminin alpha2 deficiency and abnormal glycosylation of alpha-dystroglycan. *Am. J. Hum. Genet.*, 69, 1198-1209.
30. Brockington,M., Yuva,Y., Prandini,P., Brown,S.C., Torelli,S., Benson,M.A., Herrmann,R., Anderson,L.V., Bashir,R., Burgunder,J.M., *et al.* (2001) Mutations in the fukutin-related protein gene (FKRP) identify limb girdle muscular dystrophy 2I as a milder allelic variant of congenital muscular dystrophy MDC1C. *Hum. Mol. Genet.*, 10, 2851-2859.
31. Lefeber,D.J., Schonberger,J., Morava,E., Guillard,M., Huyben,K.M., Verrijp,K., Grafakou,O., Evangelidou,A., Preijers,F.W., Manta,P., *et al.* (2009) Deficiency of Dol-P-Man synthase subunit DPM3 bridges the congenital disorders of glycosylation with the dystroglycanopathies. *Am. J. Hum. Genet.*, 85, 76-86.
32. Willer,T., Lee,H., Lommel,M., Yoshida-Moriguchi,T., de Bernabe,D.B., Venzke,D., Cirak,S., Schachter,H., Vajsar,J., Voit,T., *et al.* (2012) ISPD loss-of-function

1
2
3
4
5
6
7
8
9
10
11
12
13
14
15
16
17
18
19
20
21
22
23
24
25
26
27
28
29
30
31
32
33
34
35
36
37
38
39
40
41
42
43
44
45
46
47
48
49
50
51
52
53
54
55
56
57
58
59
60

mutations disrupt dystroglycan O-mannosylation and cause Walker-Warburg syndrome. *Nat. Genet.*

33. Cirak,S., Foley,A.R., Herrmann,R., Willer,T., Yau,S., Stevens,E., Torelli,S., Brodd,L., Kamynina,A., Vondracek,P., *et al.* (2013) ISPD gene mutations are a common cause of congenital and limb-girdle muscular dystrophies. *Brain*, 136, 269-281.
34. Manzini,M.C., Tambunan,D.E., Hill,R.S., Yu,T.W., Maynard,T.M., Heinzen,E.L., Shianna,K.V., Stevens,C.R., Partlow,J.N., Barry,B.J., *et al.* (2012) Exome sequencing and functional validation in zebrafish identify GTDC2 mutations as a cause of Walker-Warburg syndrome. *Am. J. Hum. Genet.*, 91, 541-547.
35. Vuillaumier-Barrot,S., Bouchet-Seraphin,C., Chelbi,M., Devisme,L., Quentin,S., Gazal,S., Laquerriere,A., Fallet-Bianco,C., Loget,P., Odent,S., *et al.* (2012) Identification of mutations in TMEM5 and ISPD as a cause of severe cobblestone lissencephaly. *Am. J. Hum. Genet.*, 91, 1135-1143.
36. Buysse,K., Riemersma,M., Powell,G., van,R.J., Chitayat,D., Roscioli,T., Kamsteeg,E.J., van den Elzen,C., van,B.E., Blaser,S., *et al.* (2013) Missense mutations in beta-1,3-N-acetylglucosaminyltransferase 1 (B3GNT1) cause Walker-Warburg syndrome. *Hum. Mol. Genet.*, 22, 1746-1754.
37. Lefeber,D.J., de Brouwer,A.P., Morava,E., Riemersma,M., Schuurs-Hoeijmakers,J.H., Absmanner,B., Verrijp,K., van den Akker,W.M., Huijben,K., Steenbergen,G., *et al.* (2011) Autosomal recessive dilated cardiomyopathy due to DOLK mutations results from abnormal dystroglycan O-mannosylation. *PLoS. Genet.*, 7, e1002427.
38. Yoshida-Moriguchi,T., Willer,T., Anderson,M.E., Venzke,D., Whyte,T., Muntoni,F., Lee,H., Nelson,S.F., Yu,L., Campbell,K.P. (2013) SGK196 Is a Glycosylation-Specific O-Mannose Kinase Required for Dystroglycan Function. *Science*.
39. Carss,K.J., Stevens,E., Foley,A.R., Cirak,S., Riemersma,M., Torelli,S., Hoischen,A., Willer,T., van,S.M., Moore,S.A., *et al.* (2013) Mutations in GDP-Mannose Pyrophosphorylase B Cause Congenital and Limb-Girdle Muscular Dystrophies Associated with Hypoglycosylation of alpha-Dystroglycan. *Am. J. Hum. Genet.*, 93, 29-41.
40. Brown,S.C., Torelli,S., Brockington,M., Yuva,Y., Jimenez,C., Feng,L., Anderson,L., Ugo,I., Kroger,S., Bushby,K., *et al.* (2004) Abnormalities in alpha-dystroglycan expression in MDC1C and LGMD2I muscular dystrophies. *Am. J. Pathol.*, 164, 727-737.
41. Xu,L., Lu,P.J., Wang,C.H., Keramaris,E., Qiao,C., Xiao,B., Blake,D.J., Xiao,X., Lu,Q.L. (2013) Adeno-associated virus 9 mediated FKR gene therapy restores functional glycosylation of alpha-dystroglycan and improves muscle functions. *Mol. Ther.*, 2 July 2013.

- 1
2
3
4
5
6
7
8
9
10
11
12
13
14
15
16
17
18
19
20
21
22
23
24
25
26
27
28
29
30
31
32
33
34
35
36
37
38
39
40
41
42
43
44
45
46
47
48
49
50
51
52
53
54
55
56
57
58
59
60
42. Kanagawa,M., Yu,C.C., Ito,C., Fukada,S.I., Hozoji-Inada,M., Chiyo,T., Kuga,A., Matsuo,M., Sato,K., Yamaguchi,M., *et al.* (2013) Impaired viability of muscle precursor cells in muscular dystrophy with glycosylation defects and amelioration of its severe phenotype by limited gene expression. *Hum. Mol. Genet.*, 22, 3003-3015.
43. Inamori,K., Yoshida-Moriguchi,T., Hara,Y., Anderson,M.E., Yu,L., Campbell,K.P. (2012) Dystroglycan function requires xylosyl- and glucuronyltransferase activities of LARGE. *Science*, 335, 93-96.
44. Barresi,R., Michele,D.E., Kanagawa,M., Harper,H.A., Dovico,S.A., Satz,J.S., Moore,S.A., Zhang,W., Schachter,H., Dumanski,J.P., *et al.* (2004) LARGE can functionally bypass alpha-dystroglycan glycosylation defects in distinct congenital muscular dystrophies. *Nat. Med.*, 10, 696-703.
45. Brockington,M., Torelli,S., Sharp,P.S., Liu,K., Cirak,S., Brown,S.C., Wells,D.J., Muntoni,F. (2010) Transgenic overexpression of LARGE induces alpha-dystroglycan hyperglycosylation in skeletal and cardiac muscle. *PLoS. ONE.*, 5, e14434.
46. Ackroyd,M.R., Whitmore,C., Prior,S., Kaluarachchi,M., Nikolic,M., Mayer,U., Muntoni,F., Brown,S.C. (2011) Fukutin-related protein alters the deposition of laminin in the eye and brain. *J. Neurosci.*, 31, 12927-12935.
47. Ackroyd,M.R., Skordis,L., Kaluarachchi,M., Godwin,J., Prior,S., Fidanboyly,M., Piercy,R.J., Muntoni,F., Brown,S.C. (2009) Reduced expression of fukutin related protein in mice results in a model for fukutin related protein associated muscular dystrophies. *Brain*, 132, 439-451.
48. Yamamoto,L.U., Velloso,F.J., Lima,B.L., Fogaca,L.L., de,P.F., Vieira,N.M., Zatz,M., Vainzof,M. (2008) Muscle protein alterations in LGMD2I patients with different mutations in the Fukutin-related protein gene. *J. Histochem. Cytochem.*, 56, 995-1001.
49. Ringelmann,B., Roder,C., Hallmann,R., Maley,M., Davies,M., Grounds,M., Sorokin,L. (1999) Expression of laminin alpha1, alpha2, alpha4, and alpha5 chains, fibronectin, and tenascin-C in skeletal muscle of dystrophic 129ReJ dy/dy mice. *Exp. Cell Res.*, 246, 165-182.
50. Yu,M., He,Y., Wang,K., Zhang,P., Zhang,S., Hu,H. (2013) Adeno-Associated Viral-Mediated LARGE Gene Therapy Rescues the Muscular Dystrophic Phenotype in Mouse Models of Dystroglycanopathy. *Hum. Gene Ther.*, 24, 317-330.
51. Hewitt,J.E. (2012) LARGE enzyme activity deciphered: a new therapeutic target for muscular dystrophies. *Genome Med.*, 4, 23.
52. Muntoni,F., Torelli,S., Brockington,M. (2008) Muscular dystrophies due to glycosylation defects. *Neurotherapeutics.*, 5, 627-632.

- 1
2
3
4
5
6
7
8
9
10
11
12
13
14
15
16
17
18
19
20
21
22
23
24
25
26
27
28
29
30
31
32
33
34
35
36
37
38
39
40
41
42
43
44
45
46
47
48
49
50
51
52
53
54
55
56
57
58
59
60
53. Norwood,F.L., Harling,C., Chinnery,P.F., Eagle,M., Bushby,K., Straub,V. (2009) Prevalence of genetic muscle disease in Northern England: in-depth analysis of a muscle clinic population. *Brain*, 132, 3175-3186.
 54. Gupta,A., Tsai,L.H., Wynshaw-Boris,A. (2002) Life is a journey: a genetic look at neocortical development. *Nat. Rev. Genet.*, 3, 342-355.
 55. Wood,H.B., Episkopou,V. (1999) Comparative expression of the mouse Sox1, Sox2 and Sox3 genes from pre-gastrulation to early somite stages. *Mech. Dev.*, 86, 197-201.
 56. Satz,J.S., Ostendorf,A.P., Hou,S., Turner,A., Kusano,H., Lee,J.C., Turk,R., Nguyen,H., Ross-Barta,S.E., Westra,S., *et al.* (2010) Distinct functions of glial and neuronal dystroglycan in the developing and adult mouse brain. *J. Neurosci.*, 30, 14560-14572.
 57. Holzfeind,P.J., Grewal,P.K., Reitsamer,H.A., Kechvar,J., Lassmann,H., Hoeger,H., Hewitt,J.E., Bittner,R.E. (2002) Skeletal, cardiac and tongue muscle pathology, defective retinal transmission, and neuronal migration defects in the Large(myd) mouse defines a natural model for glycosylation-deficient muscle - eye - brain disorders. *Hum. Mol. Genet.*, 11, 2673-2687.
 58. Kanagawa,M., Nishimoto,A., Chiyonobu,T., Takeda,S., Miyagoe-Suzuki,Y., Wang,F., Fujikake,N., Taniguchi,M., Lu,Z., Tachikawa,M., *et al.* (2009) Residual laminin-binding activity and enhanced dystroglycan glycosylation by LARGE in novel model mice to dystroglycanopathy. *Hum. Mol. Genet.*, 18, 621-631.
 59. Kanagawa,M., Michele,D.E., Satz,J.S., Barresi,R., Kusano,H., Sasaki,T., Timpl,R., Henry,M.D., Campbell,K.P. (2005) Disruption of perlecan binding and matrix assembly by post-translational or genetic disruption of dystroglycan function. *FEBS Lett.*, 579, 4792-4796.
 60. McDearmon,E.L., Combs,A.C., Sekiguchi,K., Fujiwara,H., Ervasti,J.M. (2006) Brain alpha-dystroglycan displays unique glycoepitopes and preferential binding to laminin-10/11. *FEBS Lett.*, 580, 3381-3385.
 61. Yurchenco,P.D., Cheng,Y.S. (1993) Self-assembly and calcium-binding sites in laminin. A three-arm interaction model. *J Biol Chem.*, 268, 17286-17299.
 62. Talts,J.F., Sasaki,T., Miosge,N., Gohring,W., Mann,K., Mayne,R., Timpl,R. (2000) Structural and functional analysis of the recombinant G domain of the laminin alpha4 chain and its proteolytic processing in tissues. *J. Biol. Chem.*, 275, 35192-35199.
 63. Sztal,T.E., Sonntag,C., Hall,T.E., Currie,P.D. (2012) Epistatic dissection of laminin-receptor interactions in dystrophic zebrafish muscle. *Hum. Mol. Genet.*

- 1
2
3 64. Brockington,M., Torelli,S., Sharp,P.S., Liu,K., Cirak,S., Brown,S.C., Wells,D.J.,
4 Muntoni,F. (2010) Transgenic Overexpression of LARGE Induces alpha-
5 Dystroglycan Hyperglycosylation in Skeletal and Cardiac Muscle. *PLoS. ONE.*, 5,
6 e14434.
7
- 8
9 65. Zhang,P., Hu,H. (2011) Differential glycosylation of {alpha}-dystroglycan and
10 proteins other than {alpha}-dystroglycan by LARGE. *Glycobiology*, 22, 235-247.
11
- 12 66. Aguilan,J.T., Sundaram,S., Nieves,E., Stanley,P. (2009) Mutational and functional
13 analysis of Large in a novel CHO glycosylation mutant. *Glycobiology*, 19, 971-986.
14
- 15 67. Li,S., Harrison,D., Carbonetto,S., Fassler,R., Smyth,N., Edgar,D., Yurchenco,P.D.
16 (2002) Matrix assembly, regulation, and survival functions of laminin and its
17 receptors in embryonic stem cell differentiation. *J. Cell Biol.*, 157, 1279-1290.
18
- 19 68. Takashima,Y., Era,T., Nakao,K., Kondo,S., Kasuga,M., Smith,A.G., Nishikawa,S.
20 (2007) Neuroepithelial cells supply an initial transient wave of MSC differentiation.
21 *Cell*, 129, 1377-1388.
22
- 23 69. Foster,H., Sharp,P.S., Athanasopoulos,T., Trollet,C., Graham,I.R., Foster,K.,
24 Wells,D.J., Dickson,G. (2008) Codon and mRNA sequence optimization of
25 microdystrophin transgenes improves expression and physiological outcome in
26 dystrophic mdx mice following AAV2/8 gene transfer. *Mol. Ther.*, 16, 1825-1832.
27
- 28 70. Sharp,P.S., Jee,H., Wells,D.J. (2011) Physiological characterization of muscle
29 strength with variable levels of dystrophin restoration in mdx mice following local
30 antisense therapy. *Mol. Ther.*, 19, 165-171.
31
32
33
34
35
36
37
38

39 Figure Legends.

40
41
42 **Figure 1 Real time gene expression analysis of FKRP in brain and muscle and histological**
43 **evaluation of FKRP_{MD} brain.** (A) I1H6 immunolabelling of haematoxylin stained coronal
44 sections of FKRP^{KD} heterozygote (A), FKRP^{KD} (B) and FKRP_{MD} (C) brains at P0. The cortical
45 disorganisation evident in the FKRP^{KD} is no longer evident in the FKRP_{MD} which now reflects
46 that seen in the FKRP^{KD} heterozygote control. I1H6 immunolabelling can be seen at the pial
47 basement membrane of the FKRP^{KD} heterozygote and FKRP_{MD} but not the FKRP^{KD}.
48
49 Immunolabelling of the pial basement membrane with a pan laminin antibody (D-F) shows the
50
51
52
53
54
55
56
57
58
59
60

1
2
3 disorganisation at the intrahemispheric fissure in the FKRP^{KD}, whereas in the FKRP_{MD} (F)
4 organisation is comparable to that of heterozygote FKRP^{KD} control (D). Scale bar in images A-D
5 are 50µm. Relative expression of FKRP (G,H). Taq man (Applied Biosystems) RT-PCR probes
6 were used to measure relative FKRP mRNA expression in brain and skeletal muscle of FKRP_{MD}
7 mice compared to age-matched wild type controls. Expression levels were normalised against
8 endogenous GAPDH mRNA expression. The percentage knock-down evident in the FKRP^{KD}
9 has been maintained in the FKRP_{MD} as a comparison with the levels in the FKRP^{KD} brain at
10 E15.5 show. Error bars represent SEM (n = 4). All samples were analysed as triplicate data sets.
11
12 * P value = < 0.05 (two tailed t-test) ** P value < 0.005. Error bars represent ± SEM (n = 4).
13
14
15
16
17
18
19
20
21
22
23
24
25
26
27
28

29 **Figure 2. Body weight and histological analysis of muscle at 6, 12 and 20 weeks.** (A) Mean
30 body weights ± SEM of male and female wildtype (white) and FKRP_{MD} (patterned) at 6 weeks
31 (male WT n=8, male FKRP_{MD} n=29; female WT n=14, female FKRP_{MD} n=12), 12 (male WT
32 n=10, male FKRP_{MD} n=17; female WT n=14, female FKRP_{MD} n=24) and 20 weeks of age (male
33 WT n=7, male FKRP_{MD} n=13; female WT n=6, female FKRP_{MD} n=12). Data were analysed
34 with a Linear Mixed Effects Model performed using SPSS Statistics (IBM Corporation, U.S.A).
35 This model showed that age was a significant factor affecting mouse body weight in both male
36 and female mice, but genotype was not a significant factor affecting male body weight (p=0.245)
37 although it was with respect to female body weight, with significance shown as follows: *0.01
38 ≤p<0.05, ** 0.001≤p<0.01. (B-K) Digital images of haematoxylin and eosin stained cryosections
39 from wildtype (B,D,F,H,J) and FKRP_{MD} (C,E,G,I,K) gastrocnemius (B-E, H-I) diaphragm (F-G)
40 and quadriceps (J-K) at 6 (B-C), 12 (D-E) and 30 (F-K) weeks of age. FKRP_{MD} muscle shows
41 evidence of inflammatory infiltrates and muscle fibre degeneration at 6 weeks of age (C), with
42
43
44
45
46
47
48
49
50
51
52
53
54
55
56
57
58
59
60

1
2
3 muscle fibre regeneration seen at 12 weeks of age (D). At 30 weeks of age, centrally nucleated
4
5 muscle fibres indicating previous regeneration cycles are seen in the FKRP_{MD} diaphragm (G) and
6
7 gastrocnemius (I). Counts of central nucleation were carried out on transverse 10µm muscle
8
9 cryosections of wildtype and FKRP_{MD} diaphragm, gastrocnemius and soleus at 12 and 30 weeks
10
11 of age - the muscle fibres with central nuclei were counted and expressed as a percentage of the
12
13 total number counted (approximately 500 for the soleus, 1500 for the diaphragm and 2000 for the
14
15 gastrocnemius). The histogram in L shows the mean percentage of centrally nucleated muscle
16
17 fibres ± SEM of wildtype (white) and FKRP_{MD} (patterned) in the diaphragm, gastrocnemius and
18
19 soleus at 12 and 30 weeks of age as indicated. This data was analysed using a General
20
21 Estimating Equations Model performed using SPSS statistics which showed that age, muscle and
22
23 genotype were significant factors affecting the percentage of centrally nucleated muscle fibres.
24
25 The output of this model is shown as a multiple line graph in M. Scale Bars represent 50µm in
26
27 B-K.
28
29
30
31
32
33
34
35
36
37

38 **Figure 3. Immunolabelling and Western blot analysis of FKRP_{MD} muscle.**

39
40
41 Transverse 10µm cryosections from 12 week old wildtype (A,C,E) and FKRP_{MD} (B,D,F) mouse
42
43 triceps were labelled with Hoescht 33342 to visualise the nuclei (A-B) and an antibody against
44
45 laminin $\alpha 2$ (C-D), with a colour composite shown in E-F. Laminin $\alpha 2$ immunolabelling was
46
47 variable in the FKRP_{MD} with small clusters of fibres showing an increase relative controls whilst
48
49 the majority of other fibres displayed either similar levels to controls or a slight decrease. Scale
50
51 bar represents 50µm. Western Blotting analysis (G) of quadriceps from wildtype and FKRP_{MD}
52
53 mice shows IHH6 labelling, present in WT mice (lanes 3,4 and 5) was absent in FKRP_{MD} mice
54
55
56
57
58
59
60

1
2
3 (lanes 1,2,6 and 7). Each lane contains an extract from individual animals. β -DG (43kDa) which
4 also acts as a loading control is shown to be unchanged in the FKRP_{MD}. The images shown in C
5 and D) are shown using a look up table from Image J to emphasise the variation in intensity of
6 laminin α 2 immunolabelling across the section. J shows the scale used.
7
8
9
10
11
12
13
14
15
16

17 **Figure 4. Laminin α 4 immunolabelling of FKRP_{MD} and wild type controls.**

18
19
20 Transverse 10 μ m cryosections from 12 week (A-B) and 30 week (C-F) old wildtype (A,C,E) and
21 FKRP_{MD} (B, D, F) diaphragm (A-D) and rectus femoris (E,F) were immunolabelled with an
22 antibody against laminin α 4. Immunolabelling with this antibody was confined to the capillaries
23 and nerves of wild type muscle, whereas immunolabelling was observed at the basement
24 membrane of small diameter fibres in the FKRP_{MD} diaphragm and rectus femoris at 12 and 30
25 weeks of age. By 30 weeks of age laminin α 4 was also evident at the basement membrane of
26 larger diameter fibres. Scale bar represents 50 μ m.
27
28
29
30
31
32
33
34
35
36
37
38
39

40 **Figure 5. FKRP_{MD} LARGE histology.** 10 μ m cryosections from FKRP_{MD} (A,C,E,G) and
41 FKRP_{MD}LARGE (B,D,F,H) diaphragm (A-B), soleus (C-D) gastrocnemius (E-F), and tibialis
42 anterior (G-H) at 30 weeks of age stained with haematoxylin and eosin (A-H). All muscles
43 showed a marked variation in fibre size, the presence of degenerative fibres infiltrated with
44 macrophages and an increase in centrally nucleated fibres relative to the FKRP_{MD}. I-K show
45 Alizarin Red labelling of wildtype (I), FKRP_{MD} (J) and FKRP_{MD}LARGE (K) diaphragm, with a
46 greater incidence of calcium deposits (red) observed in the FKRP_{MD}LARGE relative to FKRP_{MD}.
47 (L) is an image of a 30 week old FKRP_{MD}LARGE gastrocnemius, showing an example of split
48
49
50
51
52
53
54
55
56
57
58
59
60

1
2
3 muscle fibres. In images A-H and L scale bar represents 50 μ m. In I-K scale bar represents
4
5 100 μ m.
6
7
8
9
10

11
12 **Figure 6. Immunolabelling showing a decrease in IIH6, a reduction in laminin α 2 and**
13
14 **increase in laminin α 4.**
15
16

17
18 Transverse 10 μ m cryosections of the gastrocnemius (A-D) and diaphragm (E,F) of wildtype
19 (A,C,E) and FKRP_{MD}LARGE (B,D,F) mice, immunolabelled with IIH6 (antibody against
20 glycosylated α -DG) (A,B), laminin α 2 (C,D) and laminin α 4 (E,F). IIH6 and laminin α 2
21 immunolabelling was increased in the FKRP_{MD}LARGE mice relative to wildtype mice. Laminin
22 α 4 can be seen at the muscle fibre basement membrane of FKRP_{MD}LARGE mice whilst it is
23 confined to the capillaries of wild type mice. Scale bar represents 50 μ m.
24
25
26
27
28
29
30
31
32
33
34

35 **Figure 7. Ligand binding and quantitative analysis of split fibres and central nucleation.**
36

37
38 Western blot of α and β DG of WT, FKRP_{MD}, FKRP_{MD}LARGE (A) and laminin overlay assay of
39 wild type, wild type overexpressing LARGE, FKRP_{MD} and FKRP_{MD}LARGE (B). As can be seen
40 transgene expression in either the wild type or FKRP_{MD} gives rise to an increase in laminin
41 binding relative to wild type confirming that expression of the transgene led to the
42 hyperglycosylation of α -DG. The number of split fibres in the gastrocnemius of 12 week old
43 wildtype (n=3), FKRP_{MD} (n=3) and FKRP_{MD}LARGE (n=3) was quantified and is shown in a
44 histogram (C). The results of a one-tailed Mann-Whitney test are shown * 0.01 \leq p<0.05,
45 illustrating a significant increase with the overexpression of LARGE on the FKRP_{MD}
46 background. (D) Counts of central nucleation were carried out on transverse 10 μ m cryosections
47
48
49
50
51
52
53
54
55
56
57
58
59
60

1
2
3 of 12 and 30 week wildtype, FKRP_{MD} and FKRP_{MD}LARGE diaphragm, gastrocnemius and
4 soleus. Muscle fibres with central nuclei were counted and expressed as a percentage of the total
5 number counted (approximately 500 for the soleus, 1500 for the diaphragm and 2000 for the
6 gastrocnemius). The results of the Generalised Estimating Equations Statistical test are shown as
7 a multiple line graph. This model shows age, muscle and genotype are significant interacting
8 factors on the percentage of centrally nucleated muscle fibres. The FKRP_{MD} data shown in
9 Figure 2 has been included to facilitate comparisons between the FKRP_{MD} and FKRP_{MD}LARGE
10 models.
11
12
13
14
15
16
17
18
19
20
21
22
23
24
25

26 **Figure 8. *In vivo* assessment of muscle force production following eccentric contractions.**

27
28 Tibialis anterior muscles from 20 to 22 week old female FKRP_{MD} (n=8), FKRP_{MD}LARGE (n=5)
29 and wild-type (non-transgenic) mice (n=7) underwent a series of 10 eccentric contractions *in situ*
30 utilising a stretch of 15% of optimum muscle length. The force produced by FKRP_{MD} mice was
31 not significantly different to that of wild-type animals and showed no significant drop from
32 baseline. However, FKRP_{MD}LARGE mice showed a significant drop in force compared to the
33 value at contraction 2 (P<0.05 for contraction 8, P<0.01 for contraction 9 and P<0.001 for
34 contraction 10). FKRP_{MD}LARGE mice were significantly weaker than wild-type at contractions
35 7 to 10 (blue asterix symbols, * P<0.05, ** P<0.01) and weaker than FKRP_{MD} mice (red asterix
36 symbol, * P<0.05) after the tenth eccentric contraction. The mean force produced after 10
37 eccentric contractions was 118.46%, 105.83%, and 72.47 % of baseline for WT, FKRP_{MD}, and
38 FKRP_{MD}LARGE mice respectively. Values are presented as mean and S.E.M and data are
39 analysed using a Repeated Measures One way ANOVA with Tukey's *post-hoc* comparison.
40
41
42
43
44
45
46
47
48
49
50
51
52
53
54
55
56
57
58
59
60

Supplementary Figure 1

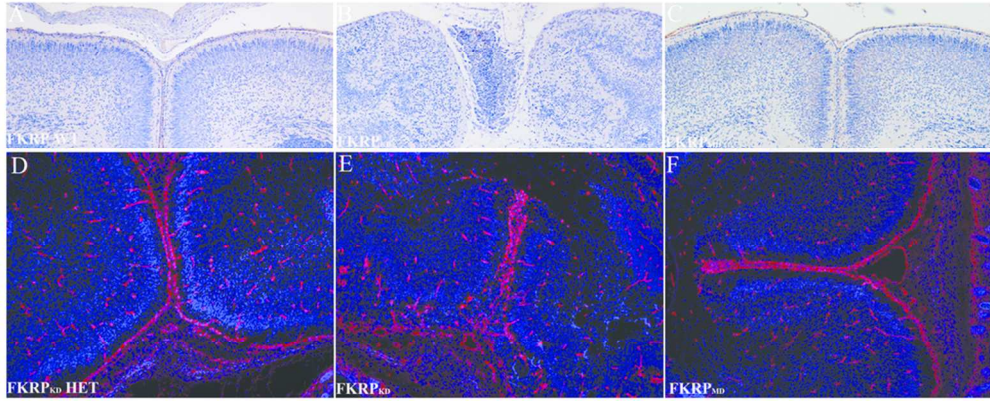
10µm cryosections from FKRP_{MD} (A,C,E,G) and FKRP_{MD}LARGE (B,D,F,H) diaphragm (A-B), soleus (C-D) gastrocnemius (E-F), and tibialis anterior (G-H) at 12 weeks of age stained with haematoxylin and eosin. All muscles showed a marked variation in fibre size and an increase in centrally nucleated fibres relative to the FKRP_{MD}

Abbreviations

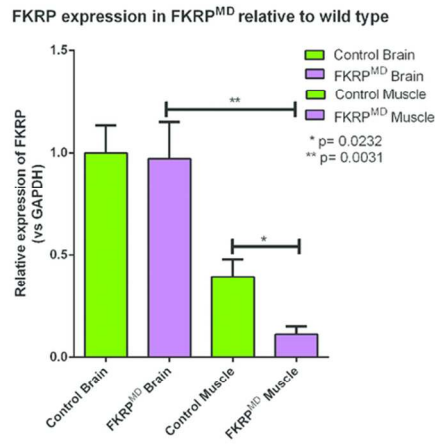
α-DG	α-dystroglycan
AAV	Adeno-Associated Virus
B3GNT1	Beta-1,3-N-Acetylglucosaminyltransferase 1
CMD	Congenital Muscular Dystrophy
DG	Dystroglycan
<i>DOLK</i>	Dolichol Kinase
DPM2	Dolichyl-Phosphate Mannosyltransferase Polypeptide 2
DPM3	Dolichyl-Phosphate Mannosyltransferase Polypeptide 3
ES	Embryonic Stem

1		
2		
3	FCMD	Fukuyama Congenital Muscular Dystrophy
4		
5		
6	FKT	Fukutin
7		
8		
9	FKRP	Fukutin Related Protein
10		
11		
12	FKRP ^{KD}	FKRP knock down
13		
14		
15		
16	FKRP _{MD}	FKRP muscular dystrophy
17		
18		
19	GalNAc	N-Acetylgalactosamine
20		
21		
22	GMPPB	GDP-mannose pyrophosphorylase B
23		
24		
25		
26	GTDC2	Glycosyltransferase-Like Domain Containing 2
27		
28		
29	ISPD	Isoprenoid Synthase Domain Containing
30		
31		
32	LARGE	Like-acetylglucosaminyltransferase
33		
34		
35	LG	Laminin globular
36		
37		
38		
39	LN	Laminin N-terminal
40		
41		
42	LGMD	Limb girdle muscular dystrophy
43		
44		
45	MDC1D	Congenital Muscular Dystrophy Type 1D
46		
47		
48	MEB	Muscle Eye Brain Disease
49		
50		
51	POMT1	Protein O-mannosyl-transferase 1
52		
53		
54		
55	POMT2	Protein O-mannosyl-transferase 2
56		
57		
58		
59		
60		

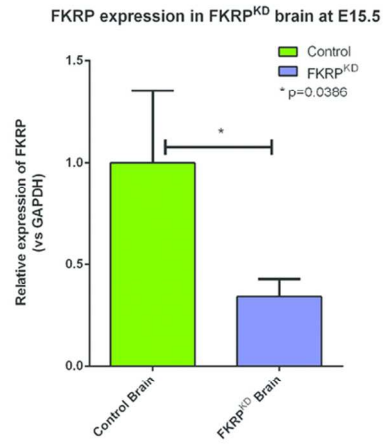
1		
2		
3	POMGnT1	Protein O-mannose beta-1,2-N-acetylglucosaminyltransferase
4		
5		
6	RT PCR	Reverse Transcriptase Polymerase Chain Reaction
7		
8		
9	Sox1	Sex determining region Y-box 1
10		
11		
12	<i>SGK196</i>	Sugen Kinase 196
13		
14		
15		
16	TA	Tibialis Anterior
17		
18		
19	TMEM5	Transmembrane Protein 5
20		
21		
22	WWS	Walker-Warburg Syndrome
23		
24		
25		
26		
27		
28		
29		
30		
31		
32		
33		
34		
35		
36		
37		
38		
39		
40		
41		
42		
43		
44		
45		
46		
47		
48		
49		
50		
51		
52		
53		
54		
55		
56		
57		
58		
59		
60		



G



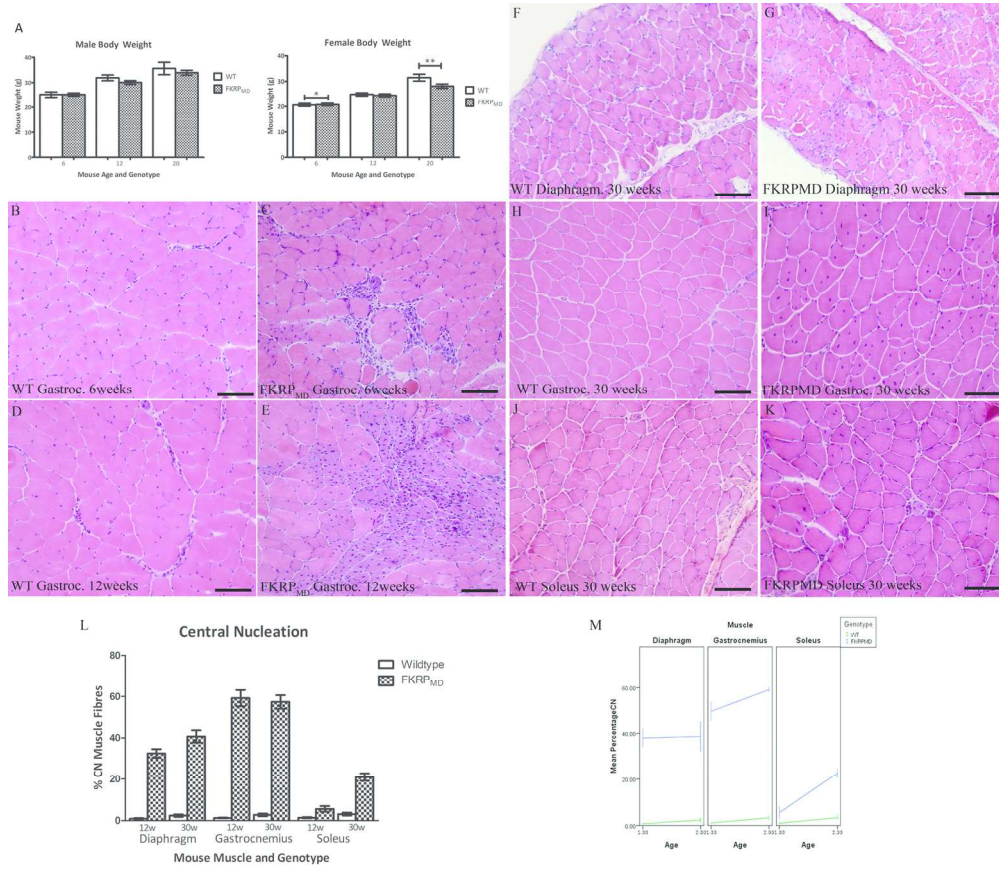
H



Real time gene expression analysis of FKRP in brain and muscle and histological evaluation of FKRPMD brain.
86x83mm (300 x 300 DPI)



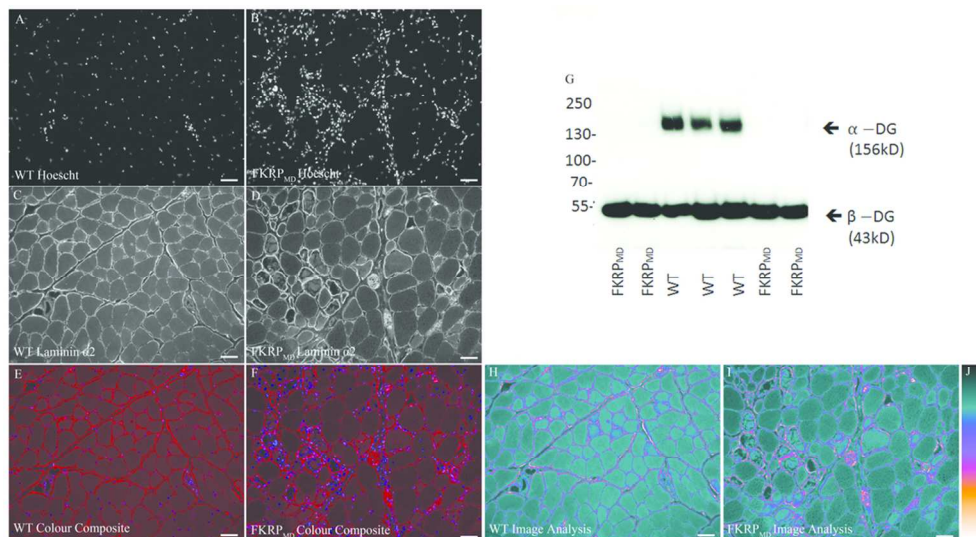
1
2
3
4
5
6
7
8
9
10
11
12
13
14
15
16
17
18
19
20
21
22
23
24
25
26
27
28
29
30
31
32
33
34
35
36
37
38
39
40
41
42
43
44
45
46
47
48
49
50
51
52
53
54
55
56
57
58
59
60



Body weight and histological analysis of muscle at 6, 12 and 20 weeks.
156x135mm (300 x 300 DPI)

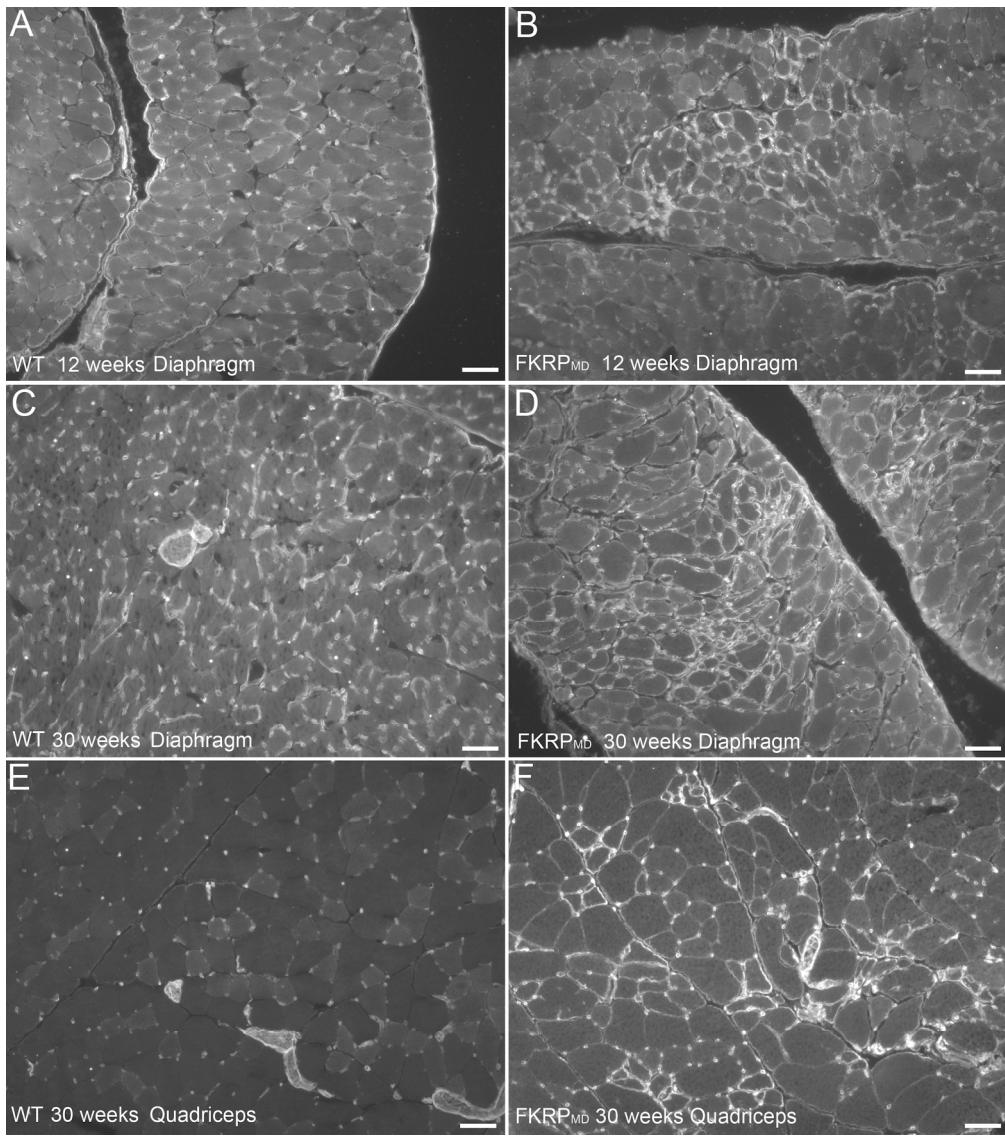
view

1
2
3
4
5
6
7
8
9
10
11
12
13
14
15
16
17
18
19
20
21
22
23
24
25
26
27
28
29
30
31
32
33
34
35
36
37
38
39
40
41
42
43
44
45
46
47
48
49
50
51
52
53
54
55
56
57
58
59
60



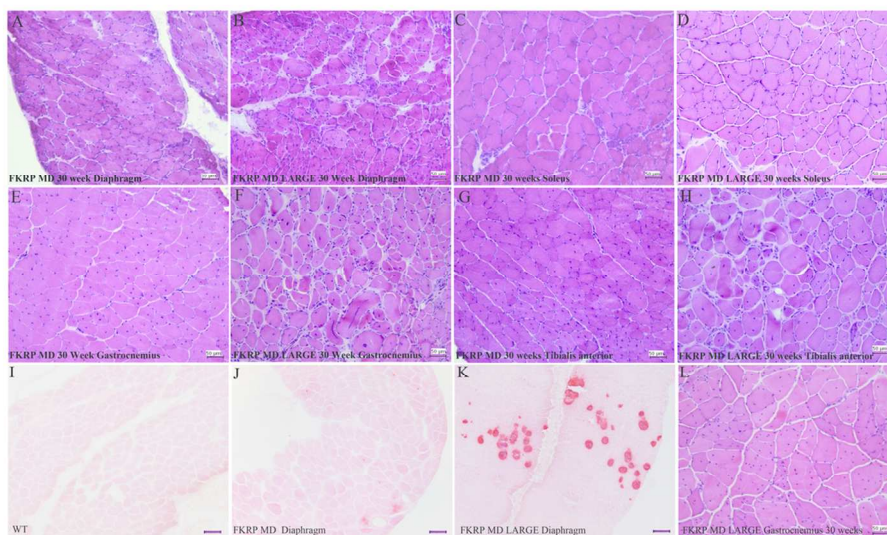
Immunolabelling and Western blot analysis of FKRPMD muscle.
97x53mm (300 x 300 DPI)

1
2
3
4
5
6
7
8
9
10
11
12
13
14
15
16
17
18
19
20
21
22
23
24
25
26
27
28
29
30
31
32
33
34
35
36
37
38
39
40
41
42
43
44
45
46
47
48
49
50
51
52
53
54
55
56
57
58
59
60



Laminin $\alpha 4$ immunolabelling of FKRPMD and wild type controls.
202x228mm (300 x 300 DPI)

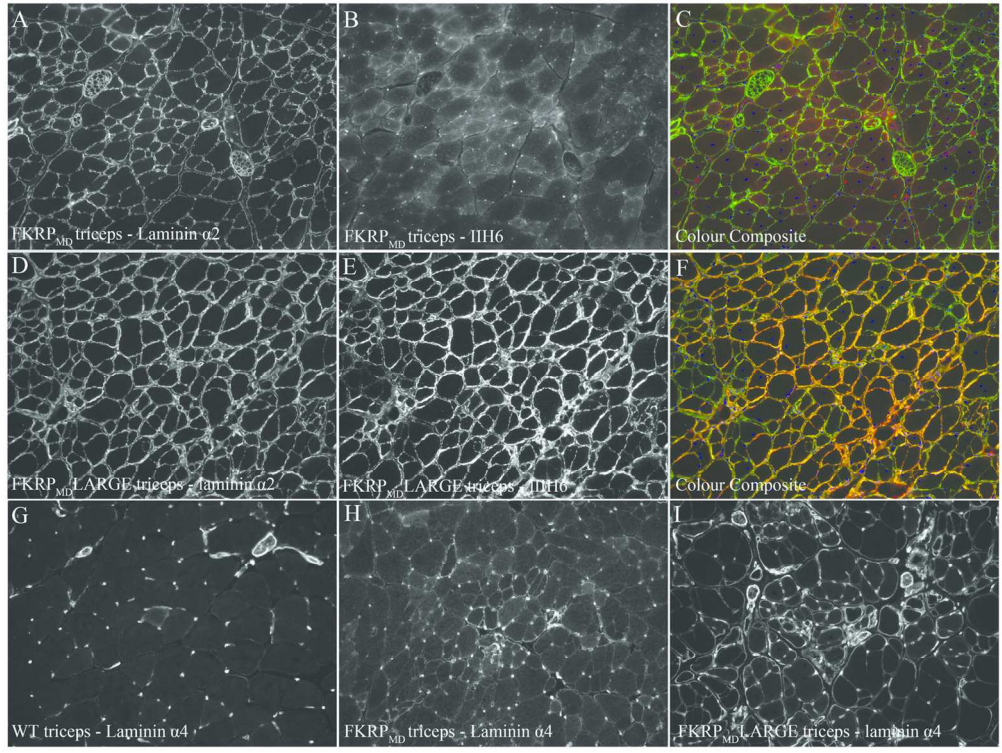
1
2
3
4
5
6
7
8
9
10
11
12
13
14
15
16
17
18
19
20
21
22
23
24
25
26
27
28
29
30
31
32
33
34
35
36
37
38
39
40
41
42
43
44
45
46
47
48
49
50
51
52
53
54
55
56
57
58
59
60



FKRPMD LARGE histology.
107x64mm (300 x 300 DPI)

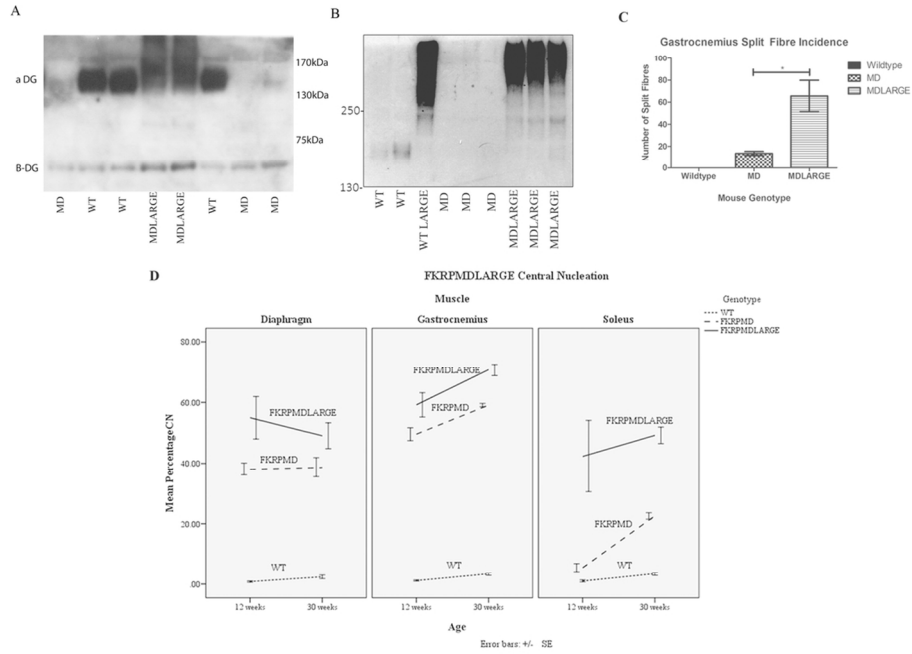
Peer Review

1
2
3
4
5
6
7
8
9
10
11
12
13
14
15
16
17
18
19
20
21
22
23
24
25
26
27
28
29
30
31
32
33
34
35
36
37
38
39
40
41
42
43
44
45
46
47
48
49
50
51
52
53
54
55
56
57
58
59
60



Immunolabelling showing a decrease in IIH6, a reduction in laminin α2 and increase in laminin α4.
135x101mm (300 x 300 DPI)

Review



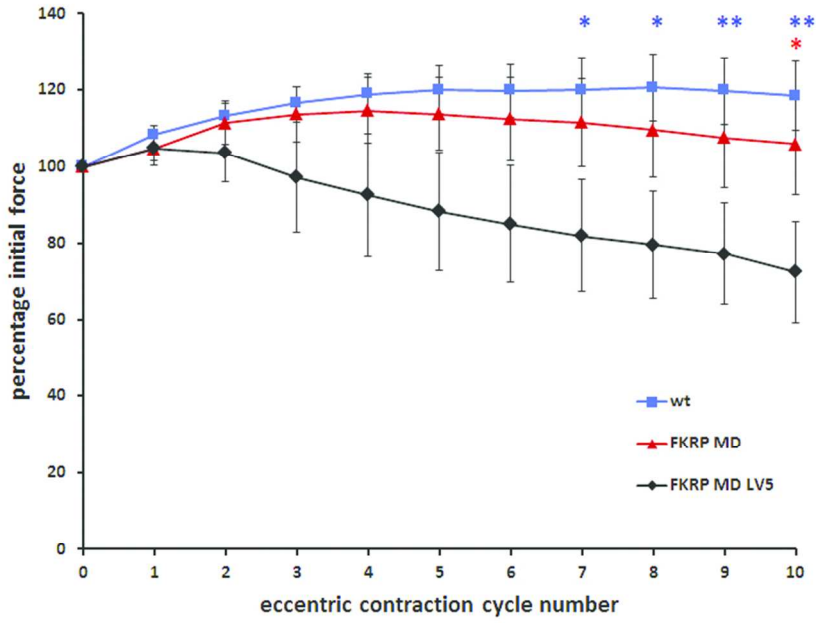
Ligand binding and quantitative analysis of split fibres and central nucleation.
108x78mm (300 x 300 DPI)

Review

1
2
3
4
5
6
7
8
9
10
11
12
13
14
15
16
17
18
19
20
21
22
23
24
25
26
27
28
29
30
31
32
33
34
35
36
37
38
39
40
41
42
43
44
45
46
47
48
49
50
51
52
53
54
55
56
57
58
59
60

1
2
3
4
5
6
7
8
9
10
11
12
13
14
15
16
17
18
19
20
21
22
23
24
25
26
27
28
29
30
31
32
33
34
35
36
37
38
39
40
41
42
43
44
45
46
47
48
49
50
51
52
53
54
55
56
57
58
59
60

Physiological analysis of *tibialis anterior* function in 20-22 week old female FKRP MD (n=8), FKRP MD LV5 (n=5) and wild type litter mates (n=7).



In vivo assessment of muscle force production following eccentric contractions.
72x56mm (300 x 300 DPI)

review

1
2
3 Reviewer: 1

4 *This is an interesting paper in which the authors create a new FKRK disease model for the*
5 *dystroglycanopathies and then test the therapeutic efficacy of LARGE overexpression in that model*
6 *using transgenic mice. Brown and colleagues had previously made an FKRK knockdown mouse model*
7 *by inserting a floxed neo cassette into intron 2 of the mouse FKRK gene. This led to reduced FKRK*
8 *gene expression and reduced functional glycosylation of dystroglycan, causing defects in cortical*
9 *migration akin to human disease with perinatal lethality. Here, they have deleted the floxed allele*
10 *that knocks down FKRK expression in the brain using Sox1-Cre to rescue knockdown in*
11 *neuroectoderm. This allows for normal brain development yet maintains an LGMD2I-like muscular*
12 *dystrophy. This alone is worthy of publication, but the authors then go on to cross this model to a*
13 *constitutively driven LARGE transgenic mouse line that they previously showed has relatively normal*
14 *muscle function but can increase alpha DG glycosylation. There are at least three groups of studies*
15 *suggesting that LARGE overexpression may increase aDG glycosylation in various forms of*
16 *dystroglycanopathy, including some where LARGE mutations are not the cause of the disease. Unlike*
17 *those studies, the work here suggests that overexpression of LARGE makes muscle disease worse,*
18 *leading to increased histopathology, particularly intracellular calcium deposits, and increase lethality*
19 *(around 27 weeks). The author's argue that the timing of LARGE overexpression may be important,*
20 *as may other matters, and so one must think more carefully about ideas utilizing LARGE for therapy*
21 *in these diseases. The concepts presented here are very worthy of publication. The work, however,*
22 *would need to be significantly revised prior to being found acceptable for HMG. The issues involved*
23 *include data presentation, data interpretation and lack of data.*
24
25
26
27
28

29
30 **We thank the reviewer for their positive and constructive comments regarding our manuscript and**
31 **have addressed their comments as follows:-**
32

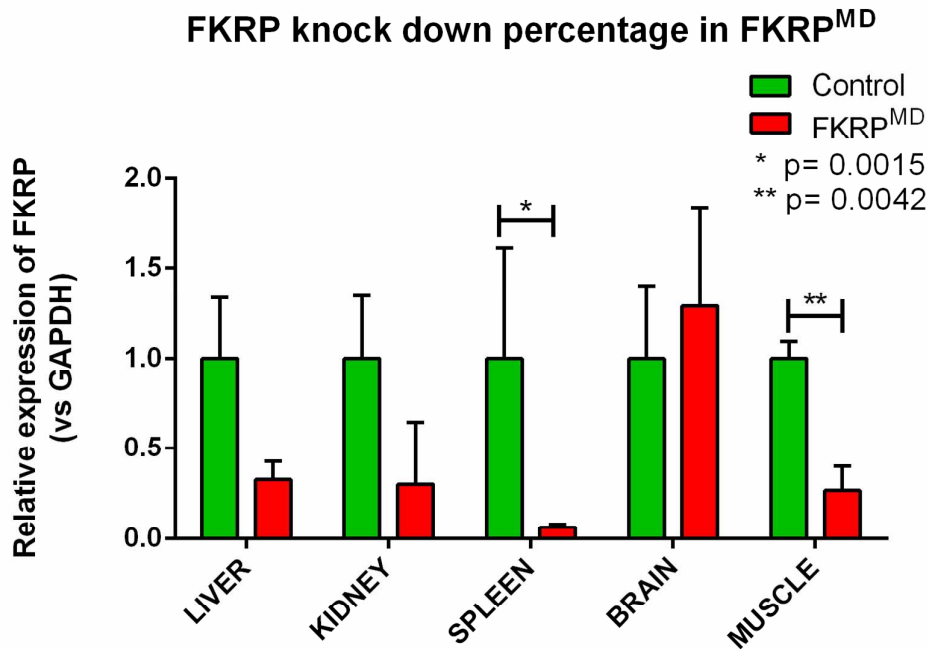
33
34 *1. Each figure is unnecessarily difficult to read. The muscles, genotypes, and ages should be labeled*
35 *on the panels to allow an easier understanding of what is presented.*
36

37
38 **We have now added the muscle, genotype and ages to each of the panels in Figures 2, 3, 4 and 5**
39 **and agree that this makes these figures much easier to understand.**
40

41
42 *2. For Figure 1, we should see much more data on the relationship between gene knockdown and*
43 *phenotype. Is FKRK expression in FKRK MD muscle lower, greater, or the same as expression in FKRK*
44 *KD muscle? This needs to be shown. Is the Sox1-Cre rescue of FKRK expression specific to brain (what*
45 *about spinal cord, heart, liver, kidney, etc)? This is particularly important, given that the authors will*
46 *later show that a Tg mice constitutively overexpressing LARGE makes disease worse.*
47

48
49 **We have now added a histogram depicting a QPCR of *Fkrp* in the brain at E15.5 in the FKRK^{KD}**
50 **mouse so that the percentage knock-down can be seen to be similar in the FKRK_{MD} and FKRK^{KD}**
51 **mice. We have also carried out similar analyses in other tissues including liver, kidney and spleen,**
52 **the results of which are shown below. As can be seen this is statistically significant in spleen, brain**
53 **and muscle but there is a trend for lower levels in the other tissues which requires more analyses**
54 **if it is to be verified given the size of the error bars. For this reason we would prefer not to include**
55 **these preliminary analyses in the paper. We have also observed that I1H6 is reduced in the heart of**
56
57
58
59
60

the FKRP^{MD}. Overall these data are consistent with what is known about the pattern of activity of the Sox1.



If *LARGE* is overexpressed everywhere, how will we know its relationship to *FKRP* in other organs if we don't know if *FKRP* is lower or not.

Whilst we agree with the referee that the knock-down of *Fkrp* in other tissues is of relevance given that *LARGE* was expressed constitutively, the focus of our study was the up-regulation of *LARGE* on a background of *FKRP* deficiency in skeletal muscle, and our paper specifically focuses on the worsening of the skeletal muscle phenotype. The overexpression of *LARGE* was achieved under the CAAGs promoter which gave rise to varying levels of *LARGE* in each tissue, with the highest levels evident in skeletal muscle - in comparison to skeletal muscle levels were approximately 4x lower in the heart and 10x lower in brain, kidney and liver (Brockington et al. PLoS One. 2010 Dec 28;5(12). The overexpression of *LARGE* in other organs relative to the levels of *Fkrp* is of obvious interest to the disease phenotype, but is beyond the remit of the present study which as the reviewer notes already includes the generation of a new model for this group of diseases and the testing of a possible therapeutic strategy.

The staining for *IH6* in the pial basement membrane needs to be more convincing. Previously, the authors have used double IF with laminin and *IH6*, and laminin and beta *DG*, to show localization at the pial BM. Why not here as well? Also, just showing *FKRP MD* and not other genotype for this just isn't convincing. Please show *FKRP KD* and *WT* for comparison, just as in other parts of the figure.

1
2
3 We have now generated a new figure which includes WT, FKRP^{KD} and FKRP_{MD} immunolabelled for
4 IIH6. We hope that the staining at the pial basement membrane is clearer as we have chosen to
5 zoom in on the cortical surface in all these images. We have used paraffin embedded sections for
6 this part of the figure due to IIH6 showing more clearly using the Dako Envision kit than it does
7 with immunofluorescence which we have used previously. As can be seen the FKRP^{KD} shows a
8 disruption of neuronal layering and an absence of IIH6 labelling at the pial basement membrane.
9 Pan laminin immunolabelling shown in the lower half of the new figure is on frozen sections of
10 FKRP^{KD} heterozygote (heterozygotes display no disease phenotype), FKRP^{KD} and FKRP_{MD}. This
11 shows clearly that the continuity of the pial basement membrane has been restored in the FKRP_{MD}
12 such that it is indistinguishable from the FKRP^{KD} heterozygote (which shows no disease
13 phenotype). We hope that this figure is now acceptable to the reviewer.
14
15
16

17
18 *3. In Figure 2, it would be better to show all of the data at different ages in the same graph, with*
19 *statistical comparisons between ages for each muscle described within the figure, and also with*
20 *statistical comparisons between genotypes.*
21
22

23 We have now revised the graph so the figure now contains one combined bar graph with the data
24 from both ages. Before our first submission we consulted a statistician and analysed our data with
25 a Generalised Estimating Equations model. This showed that age, muscle and genotype were all
26 interacting factors significantly affecting the percentage of centrally nucleated fibres. We thank
27 the reviewer for highlighting that the results of this analysis were not presented clearly so we
28 have revised the text and included a line graph, which we were advised is the best way to present
29 this analysis.
30
31
32

33
34 *4. The magnifications in Figure 3 are oddly chosen. A and B show a very low power images, where the*
35 *soleus shows IIH6 staining but the rest of the gastroc does not? This is not helpful and likely not true.*
36 *Ideally, even in the FKRP MD muscles, at high power, one should be able to show IIH6 staining in an*
37 *intramuscular peripheral nerve to demonstrate that the antibody worked. There are no clear positive*
38 *controls for staining shown here.*
39
40

41 The images we previously showed were an accurate reflection of the difference in intensity that
42 we always see in the soleus compared to the gastrocnemius. We have nonetheless removed this
43 image from Figure 3 and instead showed an image of the WT and FKRP_{MD} triceps in Figure 6
44 labelled with both laminin $\alpha 2$ and IIH6. Two nerves can clearly be seen with the laminin $\alpha 2$
45 immunolabelling but are barely detectable with IIH6 (some faint labelling is visible around the
46 endoneurium) suggesting that this is not an ideal internal control as *Fkrp* expression may not have
47 been restored in the intramuscular nerves. All sections included in this Figure were labelled at the
48 same time, collected using the same exposure times and include sections of FKRP_{MD}LARGE which
49 we hope convinces the reviewer that our staining has worked.
50
51
52

53
54 *5. The laminin alpha 2 staining is just not convincing. The authors suggest that FKRP MD muscle has*
55 *altered laminin alpha 2 staining, with higher expression in regenerating fibers and lower expression*
56 *on mature fibers. This just cannot be ascertained from what is shown. One would need co-stains*
57 *(markers of regenerating versus mature muscle) and blots to further this conclusion. Also, the title of*
58
59
60

1
2
3 *this section refers to laminin "deposition", which is only a component of overall expression shown by*
4 *staining.*
5
6

7 **We have now immunolabelled for developmental myosin as the reviewer suggests and find that**
8 **very few fibres express developmental myosin. Instead those groups of fibres showing an**
9 **apparent increase in laminin alpha 2 expression are associated with an increase in cellular activity.**
10 **We have prepared a new figure showing the Hoechst labelled nuclei together with the laminin**
11 **alpha 2 which clearly illustrates this. We have also added images using a look up table which**
12 **provides a more clear illustration of variations across the section which are much less apparent in**
13 **the control muscle. Western blots would not add any useful information regarding this variation in**
14 **laminin alpha 2 labelling due to it necessarily being based on extracts of the entire muscle. We do**
15 **nonetheless thank the reviewer for his/her comments regarding this aspect as the changes we**
16 **have undertaken have greatly improved the clarity of this figure.**
17
18
19

20
21 *6. Similarly, the laminin alpha 4 staining in Figure 4 is unconvincing. It would not be surprising to see*
22 *increased laminin alpha 4 staining in regenerating muscle that is unrelated to dystroglycan.*
23 *Dystroglycan deficient dystrophic muscles show tons of laminin alpha 4 staining. Some co-staining to*
24 *define myofiber subsets and also blots would be needed to assess increased or decreased matrix*
25 *expression.*
26
27

28 **Dystrophic muscle, including laminin α 2 deficient muscle (as referenced in the paper) shows an**
29 **altered deposition of laminin α 4, and we accept that this feature is not unique to disorders linked**
30 **to dystroglycan. In addition we do not claim that overall levels of laminin alpha 4 are dramatically**
31 **increased in the FKRP_{MD} but rather that in specific areas its distribution pattern is altered.**
32
33

34 **Further work has now shown that in the FKRP_{MD} laminin α 4 immunolabelling is identified at the**
35 **basement membrane of muscle fibres in discrete focal areas and that these are not necessarily**
36 **those which are regenerating (as defined by the distribution of developmental myosin). Instead**
37 **these areas tend to be associated with increased cellular activity as with laminin α 2**
38 **immunolabelling. The images shown of the FKRP_{MD} are representative of these areas. We have**
39 **now modified Figure 6 to show that these areas are greatly increased as is the intensity of labelling**
40 **in the FKRP_{MD}LARGE relative to the FKRP_{MD}. Western blotting is not sufficiently sensitive to be**
41 **useful to document such changes in distribution given that it is based on whole protein extracts.**
42
43
44

45 *7. Figure 5 would be much more convincing if FKRP MD and FKRP MD LARGE muscles were shown*
46 *together, size- and age-matched. The figure needs to be labeled so that it can be read without having*
47 *to go to the legend. This is the most important result in the paper, yet it is not as convincing as it*
48 *might be. It is very interesting that Alizarin red labeling is dramatically increased in the one FKRP MD*
49 *LARGE image shown in the diaphragm. The extent of this finding should be more carefully explained,*
50 *as it may be highly significant. Is this true in all muscles? Is it true only in regenerating fibers?*
51
52
53

54 **In order to allow for an easier comparison of the FKRP_{MD} and FKRP_{MD}LARGE muscles we have now**
55 **changed this image to show size and age matched images of each genotype and labelled the**
56 **panels to facilitate comparisons. For the sake of clarity we show the muscle at 30 weeks of age**
57 **and have moved all images at 12 weeks to supplementary data.**
58
59
60

1
2
3
4 We agree with the reviewer that the increased Alizarin Red staining in the FKRP_{MD}LARGE mice is
5 interesting. This increased Alizarin Red staining was observed in the 4 FKRP_{MD}LARGE mice and 3
6 FKRP_{MD}LARGE mice examined at 12 and 30 weeks of age respectively. Both the diaphragm and the
7 gastrocnemius were examined and age-matched FKRP_{MD}LARGE mice had larger deposits than
8 FKRP_{MD} mice. The deposits in the diaphragm also appeared larger than those in the gastrocnemius.
9 Alizarin Red staining detects calcium precipitates, so it is not a phenomenon that we would expect
10 be restricted to regenerating fibres. Instead we view it as another histological indicator of muscle
11 fibre degeneration which appears worse with the up-regulation of LARGE.
12
13

14
15
16 *8. Figure 7 is confusing. In A, the LN overlay, what is the difference between the last three lanes?
17 Where is the IIH6 and beta DG blot that should go along with the ligand binding data?*

18
19 We have now included Western blot of IIH6 and β dystroglycan which shows α -dystroglycan
20 hyperglycosylation in the FKRP_{MD}LARGE in the absence of any change in the molecular weight of β -
21 dystroglycan. Regarding the laminin overlay the last three lanes represent three different
22 FKRP_{MD}LARGE mice and show how consistent the laminin binding is between individuals.
23
24

25
26 *Why is LN binding lower in some of the FKRP MD-LARGE lanes than in WT LARGE?*

27
28 FKRP_{MD} mice will have an altered glycosylation pattern of α -dystroglycan relative to wildtype mice.
29 Although an up-regulation of LARGE has, as shown increased α -dystroglycan glycosylation over
30 and above that of wildtype mice, the precise arrangement of these sugar groups may be different
31 between WT LARGE and FKRP_{MD}LARGE, due to the reduction in *Fkrp* expression in the latter but
32 not the former. This may account for the altered laminin binding when comparing WT LARGE to
33 FKRP_{MD}LARGE animals on the laminin overlay.
34
35

36
37 *Equally important here is to confirm that the FKRP MD-LARGE line made does not show an increased
38 reduction in FKRP expression relative to FKRP MD. This data is not in the paper, but one assumes
39 these are not pure-bred lines from a Tg cross.*

40
41 We can confirm that these mice were not pure-bred lines from a transgenic cross, they were
42 maintained on a mixed background. The knock-down in the FKRP_{MD} is achieved via the insertion
43 of a neomycin resistance cassette in intron 2 of the *Fkrp* gene. Unpublished data from our
44 laboratory suggests that incorporation of the neo cassette into the *Fkrp* transcript leads to
45 nonsense mediated decay. Whilst it is conceivable that the percentage knock-down might differ as
46 a consequence of the genetic background; we believe that any differences between the different
47 genetic backgrounds would not be detectable in view of the very low levels of endogenous *Fkrp*.
48 Nonetheless we have added a sentence in the discussion to highlight this possibility.
49
50
51

52
53 *9. The functional data leaves a lot to be desired. Figure 9 shows force drop during eccentric
54 contractions in the TA muscle measured in situ. FKRP MD and FKRP MD LARGE mice are compared to
55 WT, with FKRP MD LARGE showing a mild (ca. 20%) decline by the 10th contraction. As WT LARGE
56 mice have been reported to have some mild physiological deficits, not showing data on these mice
57 here is will raise suspicion. The n also needs to be raised beyond 5 for the FKRP MD LARGE group.*
58
59
60

1
2
3 *Given the errors, the entire change here could be due to one animal. Some explanation is warranted*
4 *as to distribution by animal to better understand this data. It is also just odd to show physiology data*
5 *on a muscle where no pathology data are shown.*
6
7

8 **We previously tested the possibility that LARGE overexpression may alter the resistance of TA**
9 **muscles to contraction-induced injury which is the work that the reviewer refers to. In this study**
10 **the TA muscles were subjected to a series of lengthening contractions and the impact of these**
11 **repeated lengthening contractions on force generation measured over time (Brockington et al.,**
12 **PLoS One. 2010 Dec 28;5(12):Transgenic overexpression of LARGE induces α -dystroglycan**
13 **hyperglycosylation in skeletal and cardiac muscle). We reported no significant difference in**
14 **resistance to contraction-induced injury in 2 month old LARGE transgenic mice compared to**
15 **control mice although at 8 months of age, LARGE transgenic mice developed a significant**
16 **susceptibility to contraction-induced injury, as demonstrated by a 30% greater decline in force**
17 **generation compared to controls following 8 successive lengthening contractions. This work is**
18 **published, moreover the deficit was only seen in older animals and so we felt no requirement to**
19 **repeat these analyses in the present study which was based on animals at 20 weeks.**
20
21
22

23
24 **Regarding the possibility that with these error values one animal could have contributed to the**
25 **statistical significance of this result; we have now re-analysed the data removing one of the**
26 **animals in which the response was more marked relative to the others. However, there is still a**
27 **significant difference between wild type and FKRP_{MD}LARGE animals at eccentric cycle 9 (p=0.042)**
28 **and at eccentric cycle 10 (p=0.019). Our experience with these animals at this age and also data we**
29 **have at other ages indicates that the response is variable between individuals and that this should**
30 **be reported as such.**
31
32

33
34 **The physiological data was performed on the TA muscle and quite rightly the reviewer draws**
35 **attention to the fact that we failed to present the pathology of this muscle, we have therefore**
36 **now included images of this muscle in Figure 5.**
37
38

39 **Minor:**

40
41 *1. The authors need to state that Campbell and colleagues have shown that LARGE is a Xyl GlcA*
42 *tandem glycosyltransferase. They have also recently shown that SGK196 is the phosphor-mannose*
43 *transferase, not LARGE, as stated here.*
44
45

46 **In response to this very important point we have modified the paragraph on pages 3-4 to read:**
47 **“Whilst the precise pathway in which these proteins function is unclear, recent work suggests that**
48 **SGK196 is a glycosylation specific O-mannose kinase and that FKRP, FKTN, TMEM5, B3GNT1 and**
49 **LARGE all contribute to the generation of an extracellular matrix binding moiety on the resulting**
50 **phosphorylated core M3 glycan (38). The loss of matrix binding is associated with a profound**
51 **reduction in the binding of either I1H6 and/or VIA4-1 antibodies to α -dystroglycan (40)”.**
52
53

54
55 **and on page 5:**

56 **“Whilst there have been two recent reports of the successful restoration of functional**
57 **glycosylation and amelioration of the muscle pathology by AAV vectors carrying either FKRP (41)**
58
59
60

1
2
3 or fukutin (42), one of the most promising forms of therapy proposed in recent years for the
4 dystroglycanopathies is the up-regulation of LARGE; a bifunctional glycosyltransferase that
5 alternately transfers xylose and glucuronic acid to generate a heteropolysaccharide that confers α -
6 dystroglycan with its ligand binding properties (43).”
7

8
9 2. Page15, Introduction. Willers et al 2012 have shown that LARGE does not affect glycosylation of
10 some POMT1, FKRP and FKTN mutations. This should be cited and stated.
11

12
13 We have now altered the paragraph on page 5 to read as follows:-

14 “This is based on observations showing that LARGE is able to restore α -dystroglycan glycosylation
15 and functional laminin binding to cells taken from patients with congenital muscular dystrophy
16 (FCMD, MEB and WWS), seemingly irrespective of the gene involved (43). Whilst this response
17 may be dependent on the availability of O-mannosyl phosphate acceptor sites (32), this strategy is
18 still considered as being potentially useful for a wide range of patients.”
19

20
21 and on page 15:

22 “Whilst more recent work now demonstrates that the ability of LARGE to hyperglycosylate α -
23 dystroglycan is dependent on the availability of O-mannosyl phosphate acceptor sites and
24 correlates with the severity of the clinical phenotype (32); this strategy is still considered as being
25 potentially useful for a wide range of patients”.
26
27

28
29 The Willer paper has now been added to the bibliography (32).
30

31 3. Page 18 Title, “deposition” should be replaced by “expression”.
32

33
34 This change has now been made to the manuscript.
35

36 4. Page 27. The authors have not shown a reduction in O-mannosylation in their mouse model. Best
37 to eliminate that sentence.
38

39
40 We have now changed the sentence on page 27 to read “a reduction in α -dystroglycan
41 glycosylation”.
42

43
44 Reviewer: 2

45 The manuscript “The transgenic expression of LARGE exacerbates the muscle phenotype of
46 dystroglycanopathy mice” by Charlotte Whitmore et al describes some very interesting observation in
47 the FKRP mutant mouse model. The lack of FKRP expression in the CNS cause embryonic lethality, but
48 this is rescued by the removal of the neo cassette specifically in CNS, leading to the restoration of
49 functional glycosylation of alpha-DG in the CNS. The mild dystrophic phenotype in skeletal muscles of
50 the FKRPMD is a small surprise as the mice apparently completely lack functional glycosylated alpha-
51 DG. The demonstration that LARGE over-expression rescues the expression of functional glycosylated
52 alpha-DG, but results in worsening of muscle pathology is significant, implying that the strategy of
53 LARGE upregulation as a therapy to dystroglycanopathies requires careful reconsideration. This is
54 perhaps not surprising as the functions of LARGE remains poorly understood.
55
56
57
58
59
60

1
2
3 *The data presented in the manuscript are valid and mostly convincing. However, several issues need*
4 *the authors' attention.*

5
6
7 **We thank this reviewer for the positive comments on our manuscript and address his/her specific**
8 **concerns as follows:-**

9
10 *1) Demonstration the restoration of functional glycosylation of α -DG by western blots is important.*
11 *Such results can provide vital information to assess the type of glycosylation on the α -DG by the*
12 *LARGE over-expression. However, the only wb data in figure 7 is the laminin O/L. In the Figure,*
13 *signals for laminin binding can hardly be observed in WT muscles and there is no molecular marker to*
14 *define sizes of the signal. The quality of the western blot should be improved and a western blot with*
15 *IH6 should be provided for readers to understand the changes with the expression of the transgene*
16 *in comparison to the wild type functionally glycosylated α -DG.*

17
18
19
20 **We have now included a IH6 Western Blot to match the overlay and annotated the figure to show**
21 **the sizes.**

22
23
24 *2) The author described the pathology of the new FKRPMD in skeletal muscles, but there is no*
25 *description of the cardiac muscle. This is important for assessing the impact of LARGE over-*
26 *expression on lifespan. The mice as described by the authors have quite mild pathology in*
27 *diaphragm. It is therefore possible that a shortened lifespan of the FKRPMD/LARGE is the result of*
28 *transgene expression on cardiac muscle. The authors must have examined the cardiac muscle, and if*
29 *so, should present the data.*

30
31
32
33 **We have made preliminary studies of the cardiac muscle and found no histopathological**
34 **abnormalities in the FKRP_{MD}. In some of the FKRP_{MD}LARGE we did see more evidence of pathology**
35 **at 30 weeks. However, in the absence of functional data, which we considered outside of the**
36 **remit of the present paper, we did not feel that we had sufficient evidence to attribute such**
37 **changes with a role in the shortened lifespan of these mice. We agree with the reviewer that this**
38 **is nonetheless an important issue and we intend to follow this up in a subsequent study.**

39
40
41
42 *3) The reasons for FKRPMD-LARGE mice present worse phenotype than the FKRPMD mice do are not*
43 *clear. The authors put up two hypotheses. However, genetic background affects phenotype of FKRP*
44 *mutation as well. The authors should mention that the genetic background of the hybrid FKRPMD-*
45 *LARGE could also be a factor for the severer phenotype even without LARGE over expression.*

46
47
48 **Whilst the FKRP_{MD}LARGE transgenic has a different background to the FKRP_{MD} mouse histological**
49 **evaluation of wildtype LARGE overexpressing littermates on this new genetic background failed to**
50 **identify any signs of a muscle pathology, suggesting that it is an interaction between a deficiency**
51 **of Fkrp and overexpression of LARGE that is the underlying cause of the worsened phenotype.**

52
53
54 **We have therefore added the following sentences to the manuscript:**

55
56 **"Finally it should also be noted that as a consequence of the transgenic approach adopted here,**
57 **the FKRP_{MD}LARGE mice are on a different background to the FKRP_{MD} mouse. However, we consider**
58 **this an unlikely cause of the worsened phenotype since histological evaluation of wildtype LARGE**
59
60

1
2
3 **overexpressing mice on this new genetic background failed to identify any evidence of a**
4 **dystrophic pathology”.**
5

6 *For the Figure 6, the title sentence needs to be corrected by adding a , and an and. “Immunolabelling*
7 *showing a decrease in IHH6, reduction in laminin α -2, and increase in laminin α -4”.*
8
9

10 **We have now altered the figure title as suggested by the reviewer.**
11
12
13
14
15
16
17
18
19
20
21
22
23
24
25
26
27
28
29
30
31
32
33
34
35
36
37
38
39
40
41
42
43
44
45
46
47
48
49
50
51
52
53
54
55
56
57
58
59
60

For Peer Review